U.S. DEPARTMENT OF THE INTERIOR
U.S. GEOLOGICAL SURVEY

GEOLOGY AND MINERAL RESOURCES OF THE CORNUDAS MOUNTAINS, NEW MEXICO

By

C.J. Nutt, J.M. O'Neill, M.D. Kleinkopf, D.P. Klein, W.R. Miller, and B.D. Rodriquez
U.S. Geological Survey

and

V.T. McLemore
New Mexico Bureau of Mines and Mineral Resources

U.S. Geological Survey Open-File Report 97-282

*U.S. Geological Survey, DFC, Box 25046, M.S. 973, Denver, CO 80225

ABSTRACT

At the request of the BLM, over 100 square miles (260 square kilometers) in the Cornudas Mountains of southern Otero County, New Mexico, were evaluated for their potential for undiscovered mineral resources. There are three BLM-designated study areas in the Cornudas Mountains: Alamo Mountain, Wind Mountain, and Cornudas Mountain Areas of Critical Environmental Concern (ACEC). All three ACECs include scenic peaks comprised mainly of Tertiary alkaline igneous rocks that rise above the surrounding gently rolling topography. This report incorporates geological, geochemical, and geophysical data collected in 1996 by the authors as well as compilation of existing data.

The Cornudas Mountains are at the eastern edge of the Basin and Range Province and within the Tertiary Trans-Pecos magmatic belt. The area is underlain by easily eroded Permian carbonate rocks and Cretaceous clastic rocks that are intruded by more resistant alkaline plugs and sills. Permian rocks exposed are, from oldest to youngest, the Hueco, Yeso, and San Andres Formations. Outcrops of Lower Cretaceous rocks are restricted to areas near intrusions, and much of the exposed Cretaceous occurs as blocks in landslide deposits along the edges of intrusions. Intrusion of the plugs and sills caused folding and warping of the Paleozoic and Cretaceous rocks; fold axes are predominantly east-trending. Surface folding, as well as geophysical data, indicate unexposed intrusive rock underlying the Cornudas Mountains.

The Cornudas Mountains have been explored for nepheline syenite for industrial use and a resource is identified at Wind Mountain for industrial grade glass. No other exposed intrusion has potential for industrial grade glass. The area has been explored for metallic deposits associated with alkaline igneous rocks--uranium, beryllium, rare-earth elements, niobium, and gold and silver—but has low potential for these deposit types.

The geochemical environmental consequences of future mining would have minimal impact on the water chemistry of subsurface waters. Nepheline syenite in the Cornudas Mountains, if mined, has a limited buffering capacity and contains little or no pyrite or other sulfide minerals that generate acid and degrade the water.

INTRODUCTION

The Caballo Resource Area is a Bureau of Land Management (BLM) designated region that includes all of Sierra and Otero Counties, south-central New Mexico. Within this resource area of more than 21,000 square miles, nearly one fourth of the land is administered by the BLM. At the request of the BLM, over 100 square miles (260 square kilometers) in the Cornudas Mountains of southern Otero County, New Mexico were evaluated for their potential for undiscovered mineral resources. There are three BLM-designated study areas in the Cornudas Mountains; they are the Alamo Mountain, Wind Mountain, and Cornudas Mountain Areas of Critical Environmental Concern (ACEC). The three ACECs include three of eight individual peaks that comprise the Cornudas Mountains of New Mexico and Texas (Fig. 1). Because of the geologic similarity among the individual peaks and because the three ACECs are within 5 miles (8 km) of one another, this report addresses the geology, mineral resource potential, and environmental geochemistry of the whole of the Cornudas Mountains in New Mexico. The accompanying geologic map (Plate 1) covers the Cornudas Mountain 1:24,000-scale quadrangle and parts of the adjacent Alamo and McVeigh Hills 24,000-scale quadrangles on the west and east, respectively.

This report describes the geology, geophysics, and groundwater geochemistry, and assesses the mineral resource potential of the Cornudas Mountains, New Mexico. Resource potential is based on the likelihood that economic deposits of undiscovered metals and nonmetals, industrial rocks and minerals, and energy resources occur in the area.

Previous Investigations

U.S. Bureau of Mines (USBM) geologists, at the request of the BLM, independently conducted an examination of identifiable mineral occurrences in the Wind and Alamo Mountains ACECs in 1992 and 1993 (Korzeb and Kness, 1994) and in the Chess Draw area northwest of Wind Mountain in 1992 (Schreiner, 1994). The only potential mineral resource identified in these evaluations was industrial grade nepheline syenite that underlies Wind Mountain.

Previous investigations by the U.S. Geological Survey in this area are restricted to reconnaissance mapping by G.O. Bachman and associates during the compilation of the Geologic Map of New Mexico (Dane and Bachman, 1965).

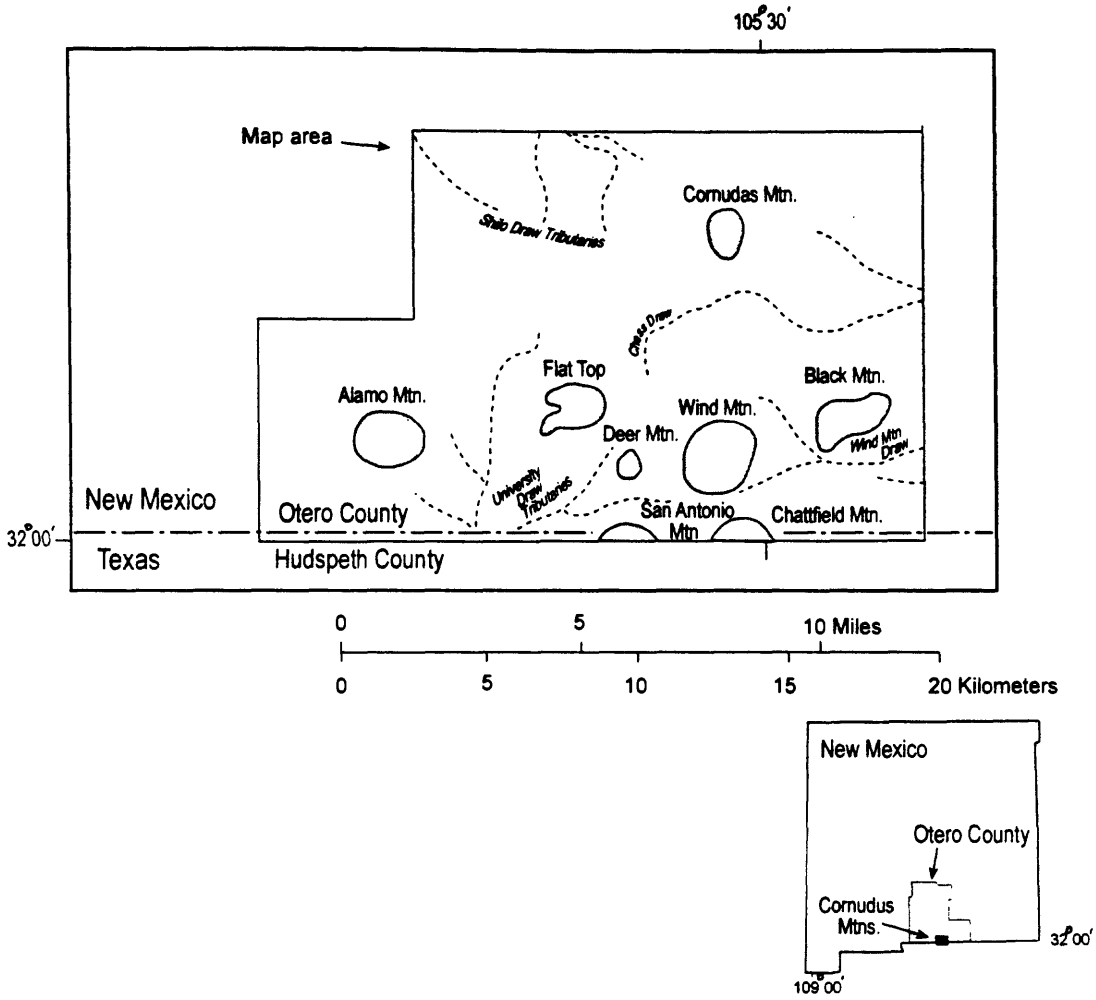

Figure 1. Index map showing the location of Cornudas Mountains New Mexico

Other published reports and unpublished theses that describe the geology of parts of the Cornudas Mountains are cited and discussed in the appropriate chapters of this report. Significant among these contributions are the theses of Timm, Zapp, and Clabaugh, all completed in 1941, discussions of mineral resources by McLemore and Guilinger (1993) and McLemore and others (1996b), analysis of groundwater geochemistry by Mayer (1995), description of Cretaceous strata by Kues and Lucas (1993), and petrologic and geochronologic analyses of igneous rocks by Barker and others (1977).

GEOLOGY

Regional Geologic Setting

The Cornudas Mountains study area is in the easternmost part of the Basin and Range province of southern New Mexico. The area is located near the center of the Otero-Diablo Platform that separates areas of Tertiary and Quaternary faulting of the Rio Grande rift on the west from the Salt Basin graben and the adjacent Guadalupe Mountains on the east (Fig. 2). The Cornudas Mountains are underlain by Permian limestone and dolomite sedimentary rocks, Cretaceous sandstone and shale, and late Eocene to early Oligocene alkaline intrusive rocks. The intrusive rocks are part of the Tertiary Trans-Pecos magmatic belt (Barker, 1977) and comprise the major peaks of the Cornudas Mountains that are, from east to west, Black, Cornudas, Wind, Chattfield, San Antonio, Deer, Flat Top, and Alamo Mountains (Figure 1 and 3, Plate 1). The Cornudas Mountains lie above the faulted, western edge of the buried Pennsylvanian Pedernal uplift; alkaline rocks apparently intruded along the pre-Permian faults and invaded Paleozoic sedimentary rocks lying unconformably on the uplifted Precambrian basement (Black, 1975, Figure 4; and this report).

Sedimentary Rocks

Permian sedimentary strata, the oldest exposed rocks in the study area, make up gently rolling hill and plain topography of this part of the Otero Platform. There are three mapable Permian formations exposed in the Cornudas Mountains and they consist of, from oldest to youngest, dark gray, cherty limestone (Hueco Formation); gypsum, shale, and limestone that is generally poorly exposed (Yeso Formation); and dolomite, dolomitic limestone, limestone, and minor clastics (San Andres Formation). Only the intermediate Yeso Formation, about 100 feet (33m) thick, is completely exposed in the map area. The base of the Hueco Formation is not exposed, and the upper part of the San Andres was removed by erosion prior to deposition of the overlying Cretaceous strata.

On the state Geologic Map of New Mexico, only two formations are shown in the Cornudas area: the gypsiferous Yeso Formation overlain by the San Andres Formation. On the Geologic Atlas of Texas map of the Van Horn-El Paso area (Barnes, 1975), three Permian formations are mapped in the southernmost Cornudas Mountains: the lowermost Hueco Formation is overlain on the east by the Permian Victorio Peak Formation and on the south and west by Permian undifferentiated Leonardian limestones. The Texas Hueco is correlative to New Mexico's Hueco and Yeso combined. The Texas Victoria Peak and Leonardian limestones are equivalent to New Mexico's San Andres. Neither the Yeso nor San Andres Formations are recognized on the Texas geologic map.

The complex stratigraphic relationships between the various Permian formations of southern New Mexico are summarized by Kottlowski (1963); stratigraphic pinchouts, abrupt lateral lithologic gradations , and stratigraphic younging from west to east, characterize the Permian section. The Yeso Formation in the southern Otero Platform grades abruptly to the south into Victorio Peak carbonate rocks which in turn grade into the dark, organic-rich calcareous mud of the Bone Springs Formation (Black, 1975). The upper San Andres Formation of New Mexico becomes younger eastward into the Guadalupe Mountains where it pinches out southward into Delaware basin sediments (Pray, 1988); the lower part intertongues with the Victorio Peak as does the underlying Yeso (Black, 1975). The three distinct Permian units mapped in the Cornudas Mountains appear to conform best with nomenclature followed in New Mexico. The lowermost limestones exposed in the map area are likely equivalents of the Hueco Limestone (Kottlowski, 1963). The Hueco is in sharp contact with the overlying, anomolously thin section of gypsum, green and red shale, and pale gray limestone of the Yeso Formation. The Yeso has not been reported south of Cornudas and appears to pinch out abruptly southward. The Yeso is overlain by a marine, near shore, shallow water deposit of carbonate and sandstone that grade upward into thin- to medium-bedded dolomitic limestone and dolomite that we correlate with the San Andres Formation. The San Andres in the western part of the map area grades laterally into Leonardian limestones, probably the Bone Springs Limestone (King, 1934) of the

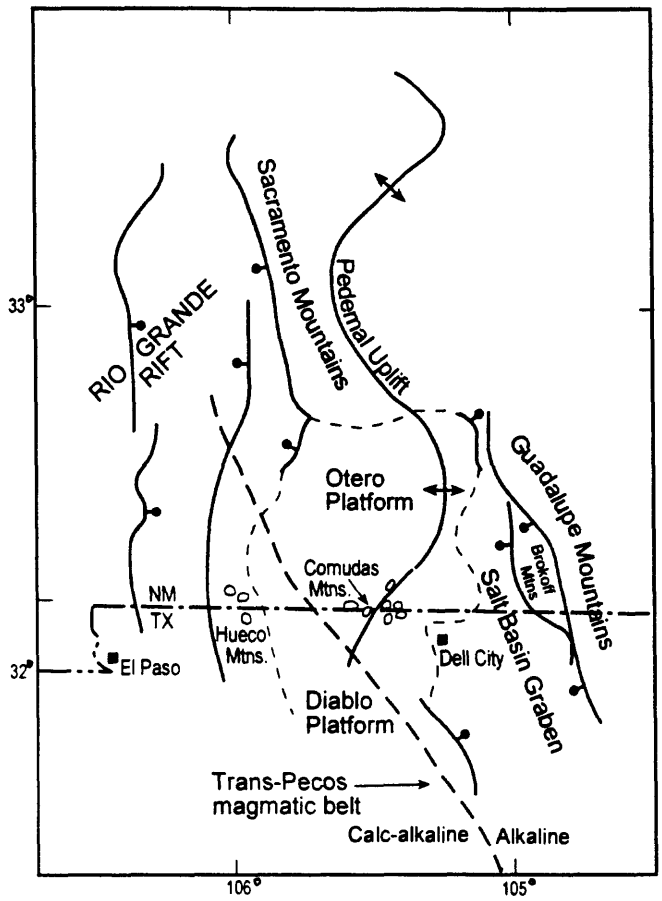

Figure 2. Generalized tectonic map of south-central New Mexico and adjacent Texas. Modified from King and Harder (1985) and Woodward and others (1975).

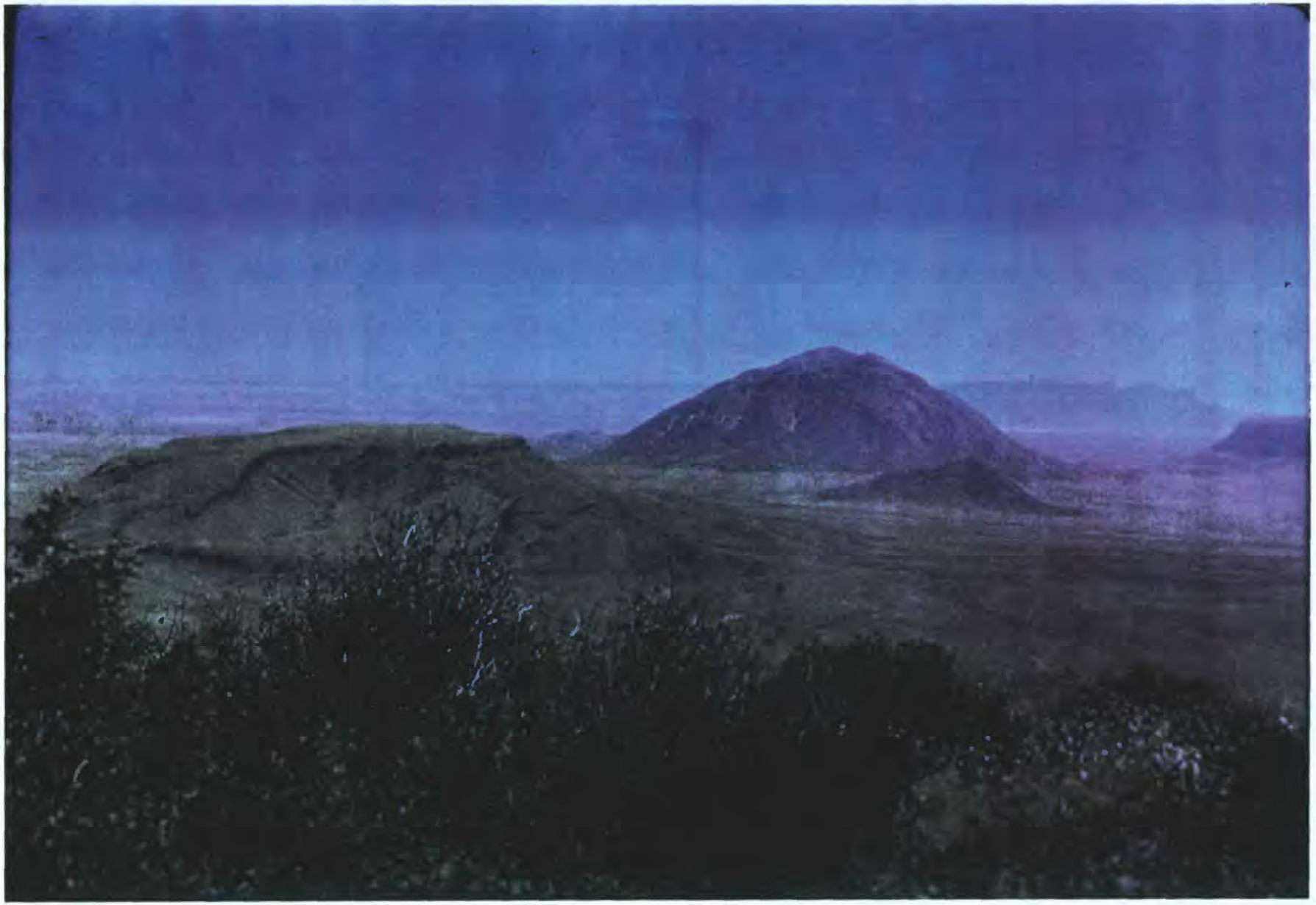

Figure 3. View of Cornudas Mountains area, looking east from crest of Alamo Mountain. Flat Top on left; Wind and smaller Deer Mountains in middle ground; north flank of Chattfield Mountain on right; Guadalupe Mountains in distance.

Diablo Platform; on the east, the formation appears to grade into the Victorio Peak carbonates, the back-ramp facies of the Capitan reef complex (Pray, 1988).

Cretaceous sedimentary rocks, also present in the map area, are exposed only where they are overlain by or adjacent to resistant igneous bodies at Alamo, San Antonio, Chatfield, and Black Mountains. Cretaceous rocks consist of basal conglomerate and associated sandstone, siltstone, and limestone and are remnants of a sedimentary section that once covered the area. The variable thickness of the lowermost Cretaceous Campagrande and Cox Formations suggest that the pre-Cretaceous depositional surface was locally irregular. Areas of Cretaceous outcrop are coincident with landslide deposits (Qls, Plate 1) and suggest that during late Tertiary erosion of the southern Otero Platform, the less resistant Cretaceous strata slumped along the edges of the more resistant igneous rocks.

Tertiary and Quaternary surficial deposits are common in the map area and consist mainly of caliche-cemented colluvium, alluvial and fluvial deposits, and ephemeral stream channel deposits. Perched gravels (QTp) of probable Pliocene-Pleistocene age are preserved adjacent to many of the peaks of the Cornudas Mountains.

Igneous Rocks

The intrusive bodies that comprise the peaks of the Cornudas Mountains represent a part of the north-northwest-trending mid-Tertiary calc-alkaline-alkaline Trans-Pecos magmatic belt of western Texas and New Mexico (McLemore and others, 1996b). The predominantly alkaline intrusive rocks of the Cornudas Mountains give way to calc-alkaline intrusives of the Hueco Mountains, about 30 miles (50 km) to the west (Fig. 2). Composition of the intrusive rocks of the Cornudas Mountains is predominantly syenite and phonolite (Plate 1). The most mafic rock is the poorly exposed augite-bearing syenite of the Chess Draw area; the most felsic rock, quartz-bearing syenite, comprises Cornudas Mountain (Barker and others, 1977). The intrusive bodies vary considerably in their shape and form, as discussed below. Flow foliation is common in all intrusive rocks and particularly well developed near contacts with adjacent sedimentary rocks. Intrusive bodies range from sills where foliation is subparallel to the enclosing, nearly flat lying sedimentary rocks (Black, Flat Top, San Antonio, Chattfield), to plug-like bodies where foliation is steep (Deer, Wind), to irregularly-shaped intrusive complexes with variable foliation where the level of erosion has exposed both feeder bodies and off-shooting sills (Cornudas, Alamo). Magnetic data discussed below indicates a major, buried intrusive body northwest of Wind Mountain and in the Chess Draw area at a depth of about 2200 feet (700 m).

Contacts between intrusive and sedimentary rock are surprisingly sharp, and the lack of anything more than sporadic and local metamorphism and alteration is striking. The Chess Draw area (Fig. 1, Plate 1) is the one area of limited altered rock that has been prospected for its mineral resource potential and is described in a later section.

Structural Geology and the Forms of Igneous Intrusions

Folds

Rocks that comprise the Otero Platform are deformed by gentle folds and minor faults (Black, 1975; Woodward and others, 1975). The relatively undeformed character of Platform rocks changes dramatically in the vicinity of the Cornudas Mountains where a complex series of gentle to steep dipping, locally asymmetric folds appear to be related to intrusion of the igneous rocks (Plate 1). Elongate domes or anticlines are centered on Cornudas Mountain and on Wind Mountain; two additional anticlines lacking exposed igneous rocks in their cores are present north of Flat Top and southwest of Alamo Mountain. Between the anticlines are a series of subparallel to obliquely-trending synclines or structural sags. The most pronounced syncline can be traced along the west side of Wind Mountain where sedimentary rocks dip as much as 60 degrees away from the peak. The complex, locally merging and commonly curvilinear patterns defined by the traces of the folds in the Cornudas Mountains bears a strong similarity to folds associated with intrusive rocks so well described by Hunt (1953) in his study of the Henry Mountains, Utah.

Cornudas Mountain in the north is within an anticline that can be traced completely across the map area; the Hueco Formation is well exposed in that part of the fold that is centered on the intrusive rocks. The trace of the anticlinal axis trends northwest on the east and folded Hueco limestones appear to extend beneath the east side of Cornudas Mountain. On the west, the fold deforms Hueco limestones that overlie the intrusion; the fold axis trends west in this area but is offset where it merges with a north-trending structural sag or syncline before reaching the western map boundary. Spatial relations between the

Cornudas Mountain intrusion and the adjacent folded rocks suggests that an elongate intrusive body underlies the entire anticlinal fold and that the exposed Cornudas intrusive is an odd shaped, sill-like body that plunges gently west, yet is bulgingly discordant on the south and southeast; Hunt (1953) might have termed this apophysis of the underlying intrusive a sphenolith.

Wind Mountain is the core of a dome in which dips of enclosing sedimentary rocks of the Hueco Formation are locally more than 60 degrees (Fig. 4). A structural sag appears to separate Deer Mountain on the west from the main part of the dome; however, Deer Mountain also intruded the Hueco and is structurally in the core of a west-trending anticlinal flexure that is a part of the Wind Mountain dome (Plate 1). The similarity in composition of Wind and Deer Mountains suggests that they are petrologically related as well. The Wind Mountain dome cannot be traced east of the peak. Wind Mountain has been interpreted as a laccolithic intrusion (McLemore and others, 1996b); however, geologic and geophysical relations mapped during this study suggest that an alternative interpretation is justified. There is no evidence that sedimentary rocks floor the intrusion; all sedimentary host rocks are strongly deformed adjacent to the intrusion and dip steeply away from the peak. Foliation within the intrusion of Wind Mountain defines a circular pattern that is mimicked by the enclosing sedimentary rocks. The aeromagnetic signature of Wind Mountain is the strongest, most prominent magnetic anomaly in the Cornudas Mountains (see Geophysical section, this report); even though topographically similar peaks are present; all other peaks are clearly floored by sedimentary rocks and, based on the magnetic signature, lack the lithologic mass of Wind Mountain. The Wind Mountain intrusion appears to be a steep-sided plug that extends downward to its intersection with a parent intrusive body that underlies the combined Wind-Deer Mountain anticlinal flexure. Hunt (1953) describes intrusive forms similar to Wind Mountain as bysmaliths.

An anticlinal, convex-northward upwarp is present north of Flat Top. The fold plunges west and terminates near Alamo Mountain; on the east it appears to merge with and become a part of the Wind-Deer Mountain anticline. A second anticlinal flexure is mapped southwest of Alamo Mountain; the fold can be traced southeast at least 7 miles (11 km) into Texas. Based on the direct correlation of anticlinal flexures and doming with known intrusive rocks, we suggest that these two additional upwarps are also cored by igneous rocks.

Synclines mapped in the Cornudas Mountains appear to be related to igneous intrusions as well. They occur as partial ring structures around Wind Mountain, as structural sags above and between buried intrusive bodies, and as paired anticline-syncline accommodation folds formed in response to dilation of intruded sedimentary rocks.

Peaks in the map area other than Cornudas Mountain and Wind Mountain do not appear to be associated with strongly deformed sedimentary rocks. Alamo Mountain, San Antonio Mountain, Chattfield Mountain, Black Mountain, and Flat Top are similar to one another in that they are concordant, clearly sills or laccoliths, and unlike Wind and Cornudas Mountains, were injected into sedimentary host rocks at or above the Permian-Cretaceous unconformity. San Antonio Mountain, perhaps the only true laccolith of the Cornudas Mountains and only partly exposed in the map area, is floored by basal Cretaceous rocks (Kues and Lucas, 1993). Chattfield Mountain, at least on the north where exposed in the map area, also is underlain by flat-lying Cretaceous strata. Black Mountain, a multiple sill complex east of Wind Mountain, was emplaced in part directly above the unconformity as well as higher in the Cretaceous section. The Flat Top sill is underlain by the San Andres Formation; no Cretaceous rocks were observed on this peak. The stratigraphic position of the unconformity east of Flat Top (north of Wind Mountain) as well as on the west (beneath Alamo Mountain) suggests that the Flat Top sill was intruded along or very near the Permian-Cretaceous unconformity.

The Alamo intrusion is perhaps the most complex of the stratigraphically higher intrusions. The intrusive body is discordant on the north where it intrudes gently west-dipping limestones of the San Andres. Along the south and west base of the peak, Cretaceous rocks are exposed. Flow foliation within the intrusive is complex. On the north flank, foliation dips steeply north; midway between the north flank and the crest of the peak, foliation becomes gently inclined to the north. Directly beneath the crest of the peak, the foliation steepens while at the crest the attitude of the foliation again becomes nearly flat lying (Plate 1). The contemporary morphology of the peak, as viewed from the northwest, reflects the abrupt changes of foliation attitude (Fig, 5), and hornfelsed Cretaceous rocks rest on the intrusion on its north side (shown as Km, Plate 1); the present exposed upper surface of the igneous rocks probably represents the exhumed upper contact of the intrusion. As such, Alamo Mountain appears to represent a steeply inclined, thick, east-trending dike on the north where it intrudes Permian strata. When the dike encountered the Permian-

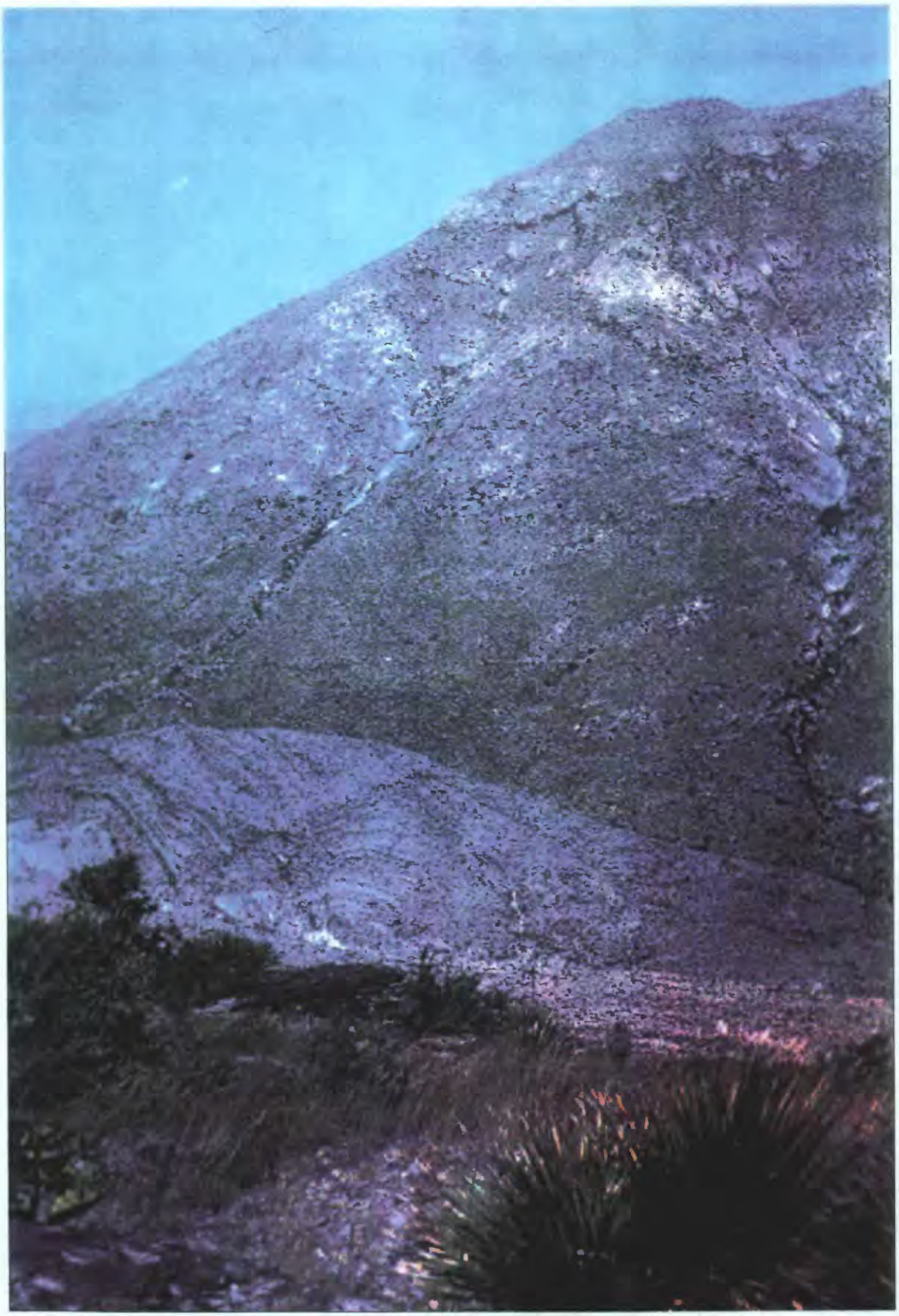

Figure 4. View of south flank of Wind Mountain showing upturned, steeply dipping Hueco Limestone that encircles the peak.

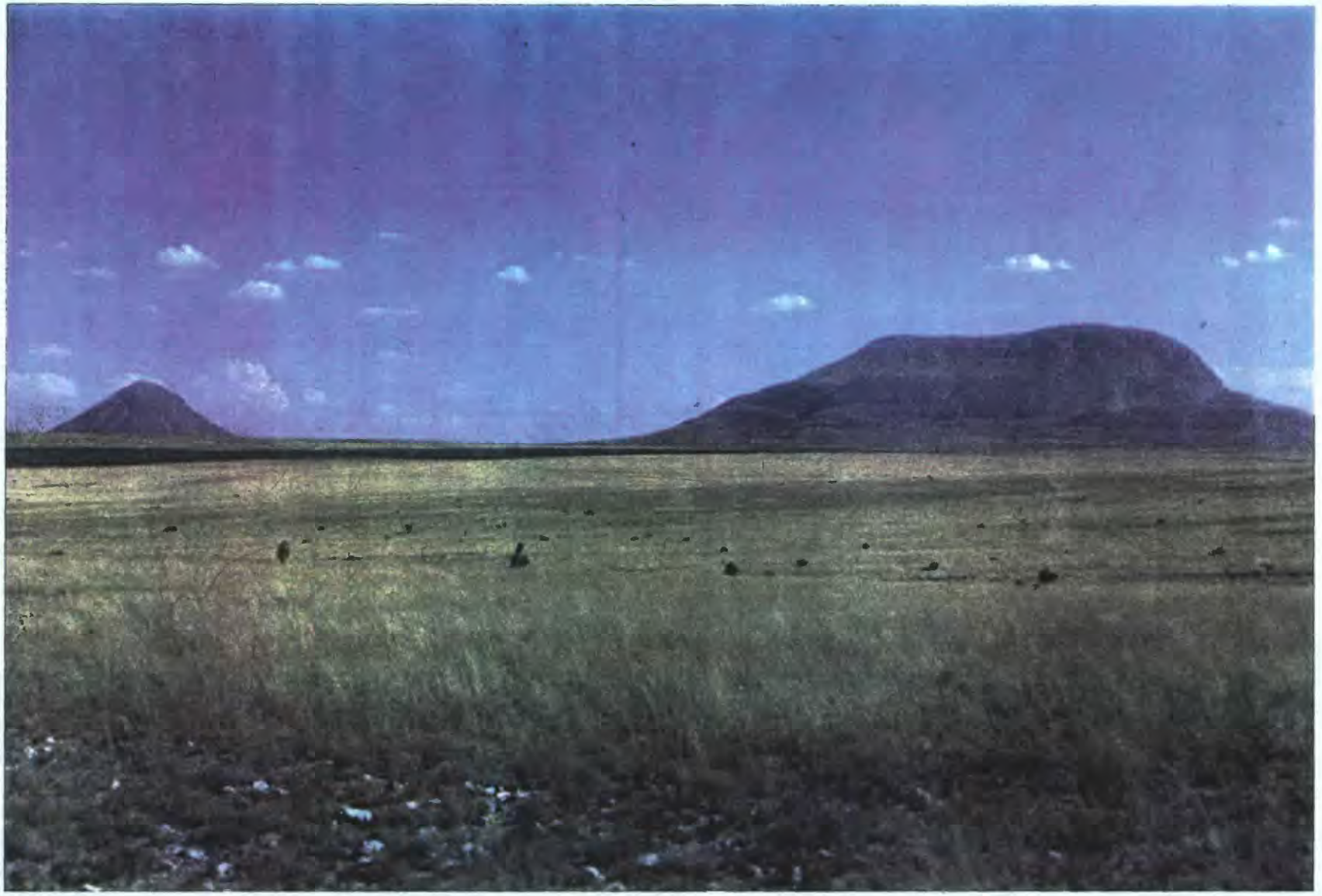

Figure 5. View of north flank of Alamo Mountain; San Antonio Mountain on left.

Cretaceous unconformity, it spread laterally to the south as a concordant intrusion before it bulged, thickened, and folded overlying Cretaceous rocks; it then concordantly invaded Cretaceous strata farther to the south before abruptly terminating at its present location. In a crude way, Alamo Mountain appears to represent an incompletely formed laccolith with its northern half undeveloped. Hunt (1953) does not describe an intrusive form quite like Alamo Mountain although he does suggest, following Daly (1914), that such an intrusion form could be called a chonolith.

Faults

The Cornudas Mountains are near the western edge of the Salt Basin graben, which is the easternmost structure related to Basin-Range tectonism and shows evidence of Quaternary fault movement (Goetz, 1980). In contrast, the Cornudas Mountains are cut by rare faults in which the offset is typically 15 or less feet (4.5 m) (Plate 1). Apparently the Cornudas Mountains are within a stable block bounded by segments of the late Cenozoic Rio Grande Rift to the west and east. Several of the small faults are intruded by dikes related to the larger intrusions of the area. We interpret the faults to have formed mainly in response to deformation of host sedimentary rocks during intrusion of alkaline rocks.

Pre-Permian Faulting

In Pennsylvanian time, New Mexico and adjacent Texas and Colorado were the sites of numerous uplifted intracratonic basement blocks of the ancestral Rocky Mountains (Kluth and Coney, 1981). Most of these uplifts and adjacent basins in New Mexico trended north; one of the larger crustal blocks, the Pedernal uplift, can be traced on the surface from central New Mexico southward into the Sacramento Mountains in eastern Otero County. From the Sacramento Mountains southward, the uplift is buried beneath Permian rocks that now underlie the Otero Platform. Basement faulting, stratigraphic pinchouts, and syntectonic sedimentary deposits associated with the uplift are best exposed in the Sacramento Mountains near Alamogordo, New Mexico (Pray, 1959, Kottlowski, 1963; Bauer and Lozinsky, 1991). To the south, similar geologic features associated with the uplift have been detected in exploratory oil wells drilled on the Otero Platform (Black, 1975).

Structure contours drawn on the top of the buried Precambrian of the Otero Platform indicate that the Cornudas Mountains are located near the western edge of the buried Pedernal uplift (Woodward and others, 1975; Foster, 1978; King and Harder, 1985). Geologic cross sections drawn across the Otero Platform by Black (1975), particularly section C-C' drawn through the northern part of the Cornudas Mountains, show the beveled top of the buried pre-Permian uplift. In section C-C', the well drilled east of the Cornudas bottomed in Permian strata resting directly on Precambrian rocks at 2280 feet (695 m) above sea level; the well on the west penetrated Permian as well as older Paleozoic rocks and encountered Precambrian basement nearly 2000 feet (610) lower, at an elevation of 481 feet (145 m) (King and Harder, 1985). The faulted, western edge of the Pedernal uplift, as shown by Black, is located between these two wells; in this cross section the Cornudas Mountains are shown as laccolithic intrusions localized along a minor fault located about 2 miles (3.5 km) west of the faulted edge of the uplift.

Geologic mapping and geophysical investigations conducted during this study suggest that the western, faulted edge of the Pedernal uplift lies beneath or west of the Cornudas Mountains. Geologic evidence for the location of the buried uplift margin is the thickness of the Permian Yeso Formation. In the Cornudas Mountains, the Yeso is only 100 feet (30 m) thick (Plate 1). In cross sections constructed by Black (1975, C-C') exploratory oil wells drilled 10 miles (16 km) east and 5 miles (8 km) northwest of the Cornudas, encountered a much thicker Yeso: about 850 feet (260 m) thick on the east and nearly 900 feet (275 m) thick on the west (King and Harder, 1985). Thinning of the Yeso to about 100 feet (30 m) in the Cornudas Mountains (Plate 1) may be due, in part, to abrupt gradation and intertonguing with the overlying San Andres; equally likely is the possibility that the formation pinches out against, over, and across an elevated Precambrian high—the uplifted Pedernal massif. Abrupt thickening of the Yeso to the west, and the fact that the entire Cambrian through Pennsylvanian section, encountered in the wildcat well, rests directly on Precambrian rocks that are nearly 2000 feet (610 m) deeper than to the east of the Cornudas Mountains, suggests that the major west-bounding fault of the Pedernal uplift is more correctly interpreted to be located west of or beneath the Cornudas Mountains.

Geophysical evidence for an abrupt change in the character of the subsurface rocks lies in aeromagnetic anomalies and audio-magnetotelluric soundings conducted across the Cornudas Mountains, as discussed below in the Geophysical section. The intrusive rocks in the subsurface of the Cornudas

Mountains appear to be concentrated at or near the unconformity between the sedimentary rocks and the underlying Precambrian crystalline basement. That unconformity is interpreted from the anomaly data to be about 2,200 feet (670 m) beneath the surface and at an elevation of about 3000 feet (915 m) above sea level. Similarly, ATM soundings detected highly resistive rocks directly east of the Cornudas Mountains that contrast markedly with a layered rock sequence detected on the west. The interpretation offered here is that the Precambrian basement is much nearer the surface directly east of the Cornudas Mountains than on the west.

In their basement structure contour map of the Otero Platform, King and Harder (1985, Fig 5) have drawn a major fault in the area of the Cornudas Mountains. Projection of the trace of that fault to the surface places it between Alamo and Wind Mountains. We would amend their structure contour map only by extending the 1500 (460 m), 2000 (610 m) and 2500 (765 m) foot basement contours farther south, beneath the Cornudas Mountains and into Texas, as shown in Figure 6a. We would amend Black's cross section C-C' to show elevated Precambrian basement directly beneath the Cornudas Mountains and suggest that the intrusion of these rocks, rather than being controlled by a relatively minor fault, was controlled by a major fault or fault system located along the western margin the Pedernal uplift (Fig. 6b).

GEOPHYSICS

Aeromagnetic and Gravity Anomaly Maps

Aeromagnetic and gravity anomaly maps (Figs. 7 and 8) were compiled for southern Otero County, New Mexico and northern Hudspeth County, Texas, from reconnaissance data that are available in the public domain. The aeromagnetic data were obtained, courtesy of the Geophysics Department, University of Texas-El Paso, from compilations of data collected during the National Uranium Resources Evaluation (NURE) program of the Department of Energy (Geometrics, Inc., 1983; Carson Helicopters, Inc., 1981). The NURE data were collected along east-west flight lines spaced 6 miles (about 10 km) apart for the Carlsbad 1:250,000 quadrangle (northeast of Lat. 32° N and Long. 106° W) and 3 miles (about 5 km) apart for the Van Horn 1:250,000 scale quadrangle (southeast of Lat 32° N and Long. 106° W). Flight altitudes were 400 feet (about 120 m) above terrain. Data reduction and merging of the NURE surveys are described by Keller and others (1983). The broad flight line spaced data are adequate for regional geologic studies and of some value for mineral resource assessment studies of the igneous intrusions of the Cornudas Mountains (Fig. 7).

The gravity data were compiled from non-proprietary data obtained from the National Imagery and Mapping Agency (NIMA) and are distributed by the National Oceanic and Atmospheric Administration (NOAA) at the National Geophysical Data Center (NGDC), Boulder, Colorado. During field work in September 1996, 11 new gravity stations were read in the vicinity of the Cornudas Mountains in order to better constrain the gravity interpretations. The reference base used was DOD 479-1 located at the Kidd Observatory, University of Texas at El Paso. The gravity data were reduced using standard USGS procedures (Bankey and Kleinkopf, 1988).

Geophysical Patterns

The total-intensity aeromagnetic map (Fig. 7) shows north- to northwest-trending patterns roughly parallel to known structures of Laramide and Basin and Range tectonism (Goetz, 1985). Prominent aeromagnetic anomalies are assumed to reflect Precambrian crystalline basement lithologies as well as younger igneous intrusive rock that may occur at basement level, within the sedimentary section, or exposed at the surface. For example, a prominent positive aeromagnetic anomaly is associated with igneous intrusions in the Cornudas Mountains. A string of northwest-trending positive and negative anomalies (probably typical dipolar pairs) that cross the New Mexico state line about 18 miles (30 km) east of the Cornudas Mountains is interpreted to reflect near-surface intrusions of syenite composition, as suggested by the syenite at Round Mountain (V.T. McLemore, oral commun., 1996), which outcrops along the anomaly trend east of Dell City. The location of the igneous intrusions may have been controlled by a northwest-trending fracture zone in the crystalline basement.

The Bouguer gravity anomaly map (fig. 8) displays similar north- to northwest-trending anomaly trends. Several positive aeromagnetic highs are observed to coincide with the gravity gradient zone along the flank of the broad gravity high roughly centered at Round Mountain, including a narrow extension of

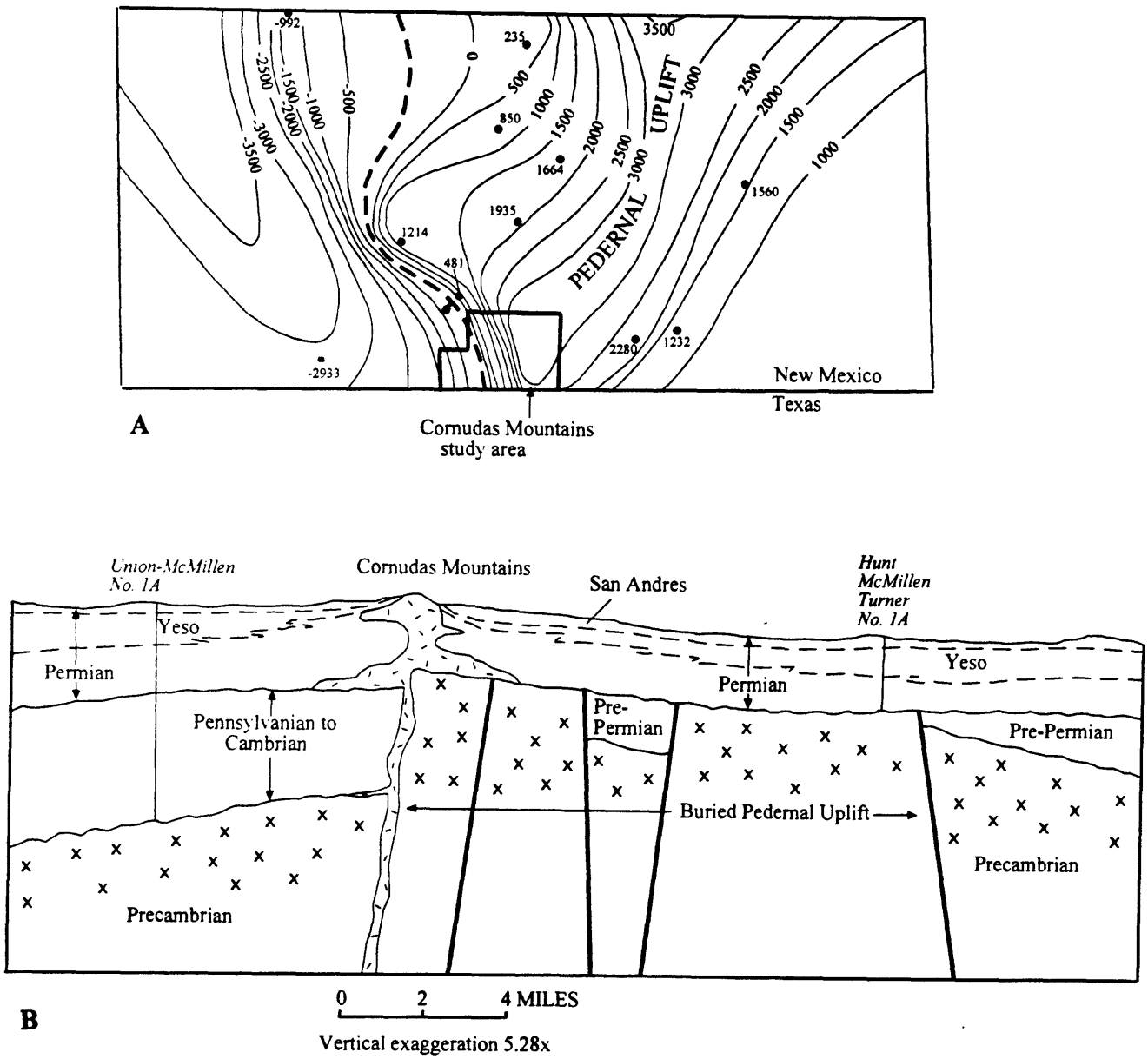

Figure 6. (a) Structure contour map on top of Precambrian basement showing location of buried Pedernal landmass with respect to Cornudas Mountains (modified from King and Harder (1985); Contour interval 500 feet; Datum: Mean Sea Level (b) Diagrammatic east-west cross section of Cornudas Mountains area showing interpreted position of Cornudas Mountains with respect to buried faults the mark the west flank of the Pedernal landmass (modified from Black, section C-C', 1975).

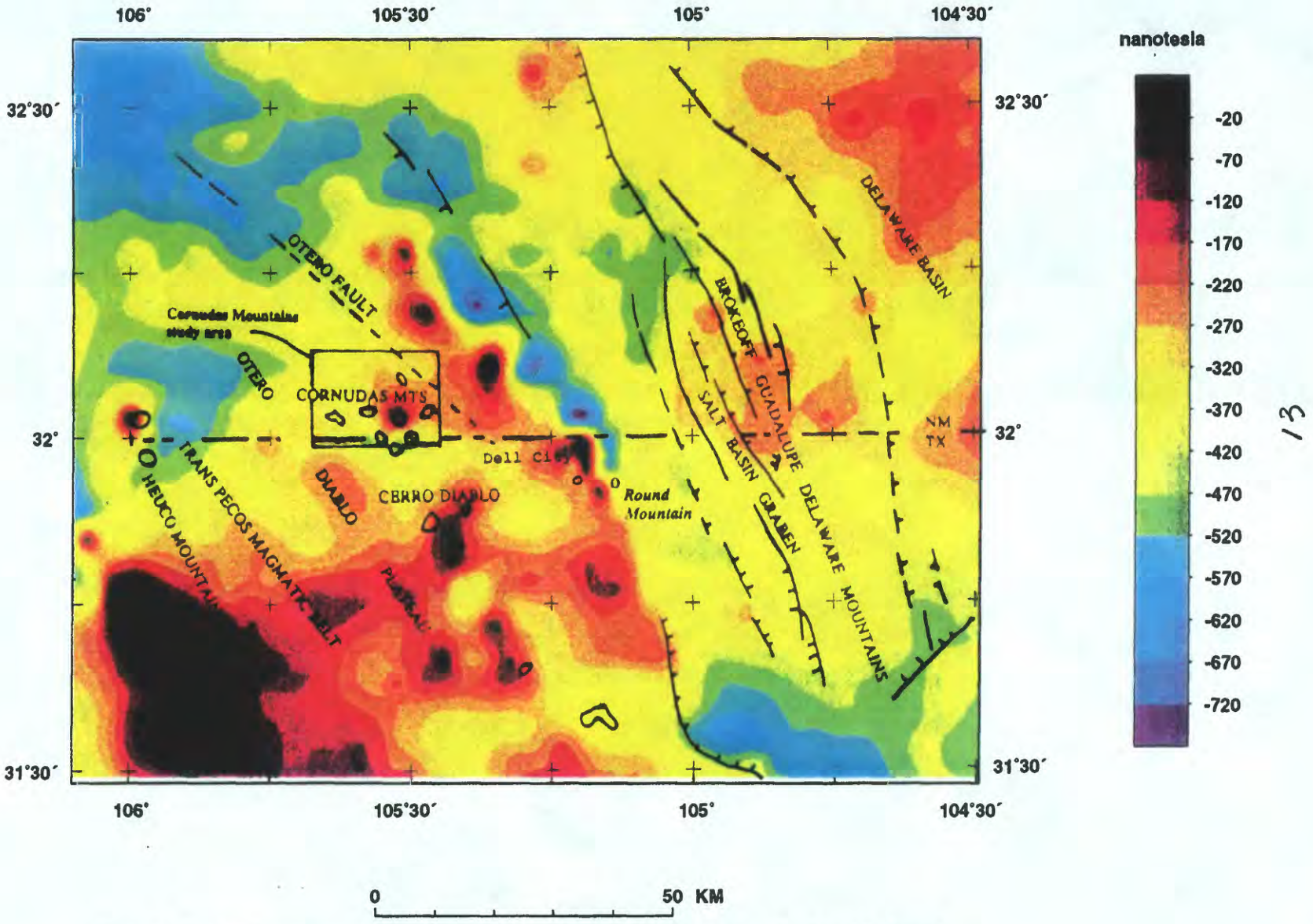

Figure 7. Regional aeromagnetic map, southern Otero County, New Mexico, and northern Hudspeth County, Texas. Contour interval 50 nanotesla. Mountain peaks in vicinity of study areas shown as heavy irregular circular features. For survey specifications, see Keller and others (1983). Faults are from Goetz (1985) and Woodward and others (1975).

Figure 8. Regional Bouguer gravity anomaly map, southern Otero County, New Mexico, and northern Hudspeth County, Texas. Contour interval 3 milligals. . Mountain peaks in vicinity of study areas shown as heavy irregular circular features. For survey specifications, see Keller and others (1983). Faults are from Goetz (1985) and Woodward and others (1975).

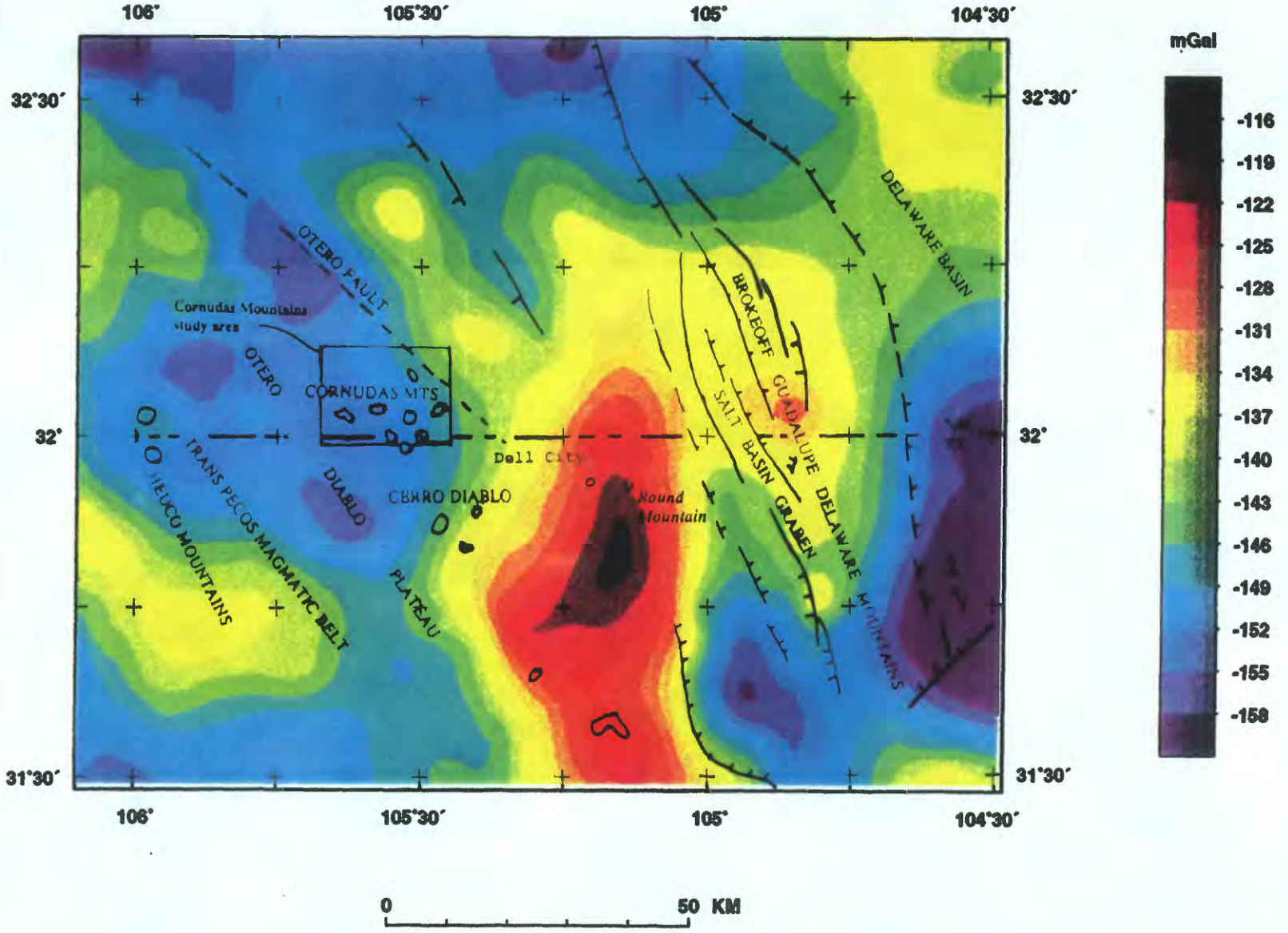

this high to the northwest of Round Mountain. This gradient zone may reflect a contact between different basement lithologies and indicates a zone of crustal weakness that accommodated placement of igneous intrusions. The northwest-trending gravity high is interpreted to reflect dense rocks in the Precambrian basement complex. An alternative interpretation is that the gravity high reflects a northwest-trending string of postulated syenite intrusions injected into less dense sedimentary rocks. However, the syenite intrusions of the Cornudas Mountains do not exhibit gravity highs, but rather correlate with low gravity (Fig 8). The Otero fault, described by Goetz (1985) as a Paleozoic transform fault, may extend southeast into Texas on the basis of lineations in the aeromagnetic anomalies. The Otero-Diablo Plateau is expressed in the gravity data as a broad gravity low. In the southwestern part of region, mostly covered by sedimentary rocks, areas of high gravity and aeromagnetic intensity probably reflect buried igneous intrusions and metamorphic rocks (Keller and others, 1983).

Cornudas Mountains ACEC

The Cornudas Mountains igneous intrusions, largely of syenite composition (Plate 1), exhibit a prominent positive magnetic anomaly centered near Wind Mountain on the residual aeromagnetic map (Fig. 9). The residual anomalies were calculated by removing a first order polynominal surface from the total-intensity magnetic field. The residual anomaly suggests that the syenite intrusions at Wind Mountain are underlain by a large igneous intrusion that was emplaced near the level of Precambrian crystalline basement rocks and centered just northwest of Wind Mountain. Measurement of anomaly gradients using a method developed by Vacquier, Steenland, Henderson, and Zietz (1951) suggest that the depth to this mass is about 2,200 feet (670 m), which is in general agreement with depth to basement published by Woodward (1975). The exposed laccoliths and sills that form the isolated peaks of the Corundas Mountains are likely apophyses associated with the main mass of igneous intrusive rock near basement level.

The aeromagnetic flight lines across the Cornudas Mountains are spaced 6 mi (10 km) apart (Fig. 9). With this wide spacing of flight lines, most of the individual laccoliths and stocks are not resolved, although as shown in the NURE quadrangle reports (Geometrics, Inc.,1983; Carson Helicopters, Inc., 1981), the flight profiles that pass along the south side of Wind Mountain and Alamo Mountain exhibit local high frequency positive spikes that are not too small to be resolved on the residual aeromagnetic map (fig. 9). The main residual aeromagnetic anomaly centered just northwest of Wind Mountain tails off to the south-southwest and forms a high of nearly 100 nT amplitude at San Antonio Mountain just south of the New Mexico-Texas state line. The flight profile at San Antonio Mountain shows a sharp high amplitude positive spike (Geometics, Inc., 1983) which corroborates the 100 nT shown on the map (Fig. 9). This same flight line in Texas crosses the north edge of Washburn Mountain and the south edge of Chatfield Mountain, but the flight profile shows only correlative faint blips that are too small to be plotted on the magnetic map.

On the regional Bouguer gravity anomaly map (Fig. 8), the Cornudas Mountains are located on the edge of a gravity re-entrant along the southwest flank of a prominent northwest-trending gravity high that was discussed under the section on geophysical patterns. The larger scale Bouguer gravity anomaly map of the study area (Fig.10) shows detail of the gravity re-entrant and the change of gravity gradient approaching the Cornudas Mountains. The gravity control consists of 31 stations for the map area (Fig 10) and the distribution of stations is adequate to define the major gravity features. The Bouguer gravity anomaly map (Fig. 10) shows that the regional gradient decreases southwesterly across the study area from about -142 mGal in the northeast to about -153 in the southwest. To depict the gravity field after removing this southwest gradient, a sloping plane surface was subtracted from the Bouguer anomaly data. The resulting residual anomaly maps portrays the area of flattened gradient and gravity re-entrant as a residual low that is gord-like in shape as defined by the 0 mGal contour. The peaks of the Cornudas Mountains occur mainly in a circular pattern within the 0 mGal contour, except for Alamo Mountain, which is a few km west. This residual low is inferred to reflect approximately a mass, likely syenite, that occurs at or just above the crystalline basement level. The gravity low results from an average negative density contrast between the syenite and adjacent Precambrian gneiss, and perhaps, with some influence from the overlying high density Paleozoic carbonate rocks.

The gravity control is not sufficient to detect subtle anomalies that might be associated with surface structure. From the geologic map (Plate 1), axes of two anticlines and a syncline that pass nearly east-west across the area are plotted on the aeromagnetic and gravity anomaly maps of the study area (Figs. 9, 10, and 11). The correlations of interest are on the residual gravity anomaly map, ie., the east-west

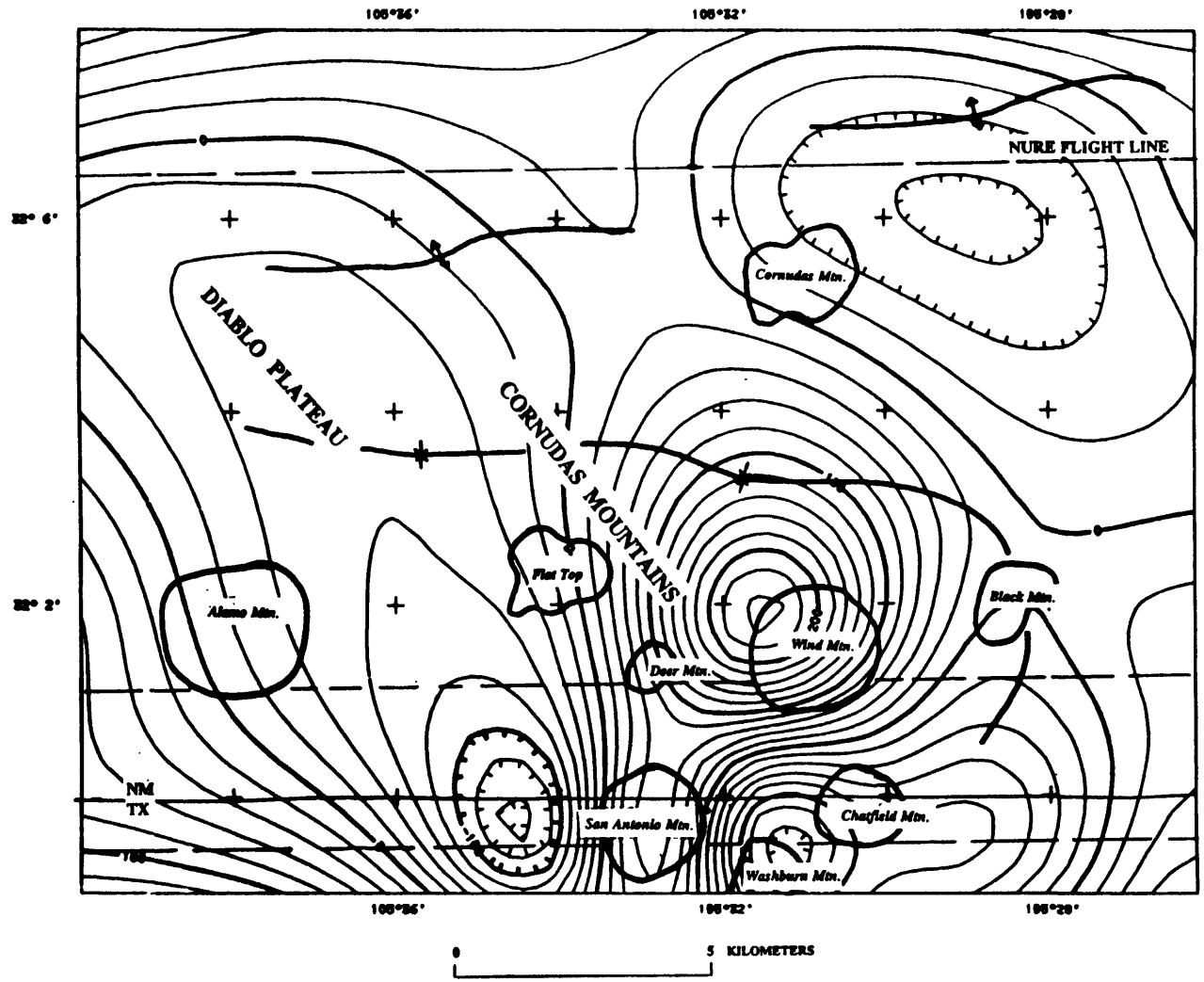

Figure 9. Residual aeromagnetic anomaly map of the Cornudas Mountains study area, southeastern Otero County, New Mexico, and northeastern Hudspeth County, Texas. Contour interval 20 nanotesla. Aeromagnetic flight lines shown by dashed lines.

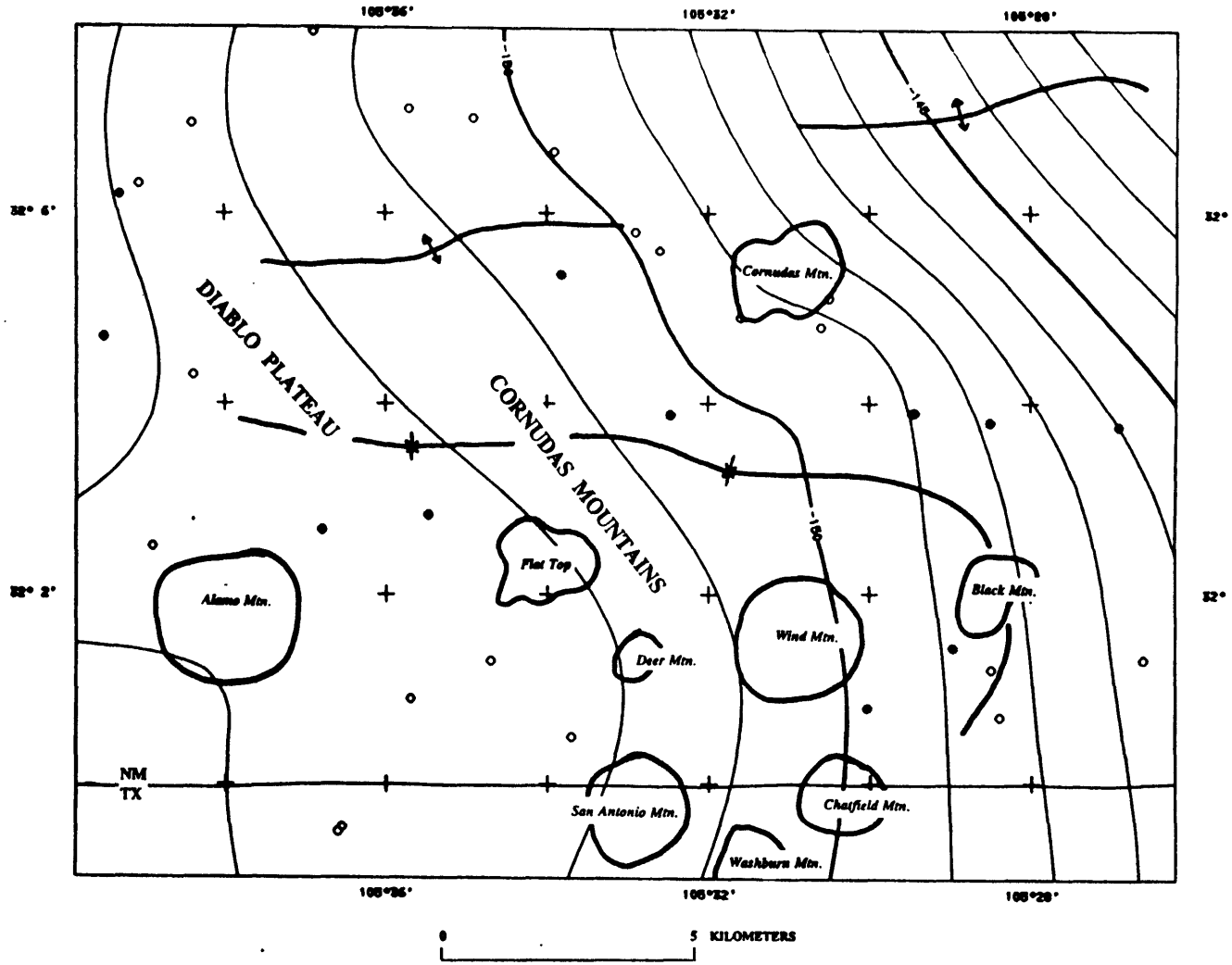

Figure 10. Bouguer gravity anomaly map of the Cornudas Mountains study area, southeastern Otero County, New Mexico, and northeastern Hudspeth County, Texas. Contour interval 2 milligals. Gravity control shown by small open circles; newly collected control by solid circles.

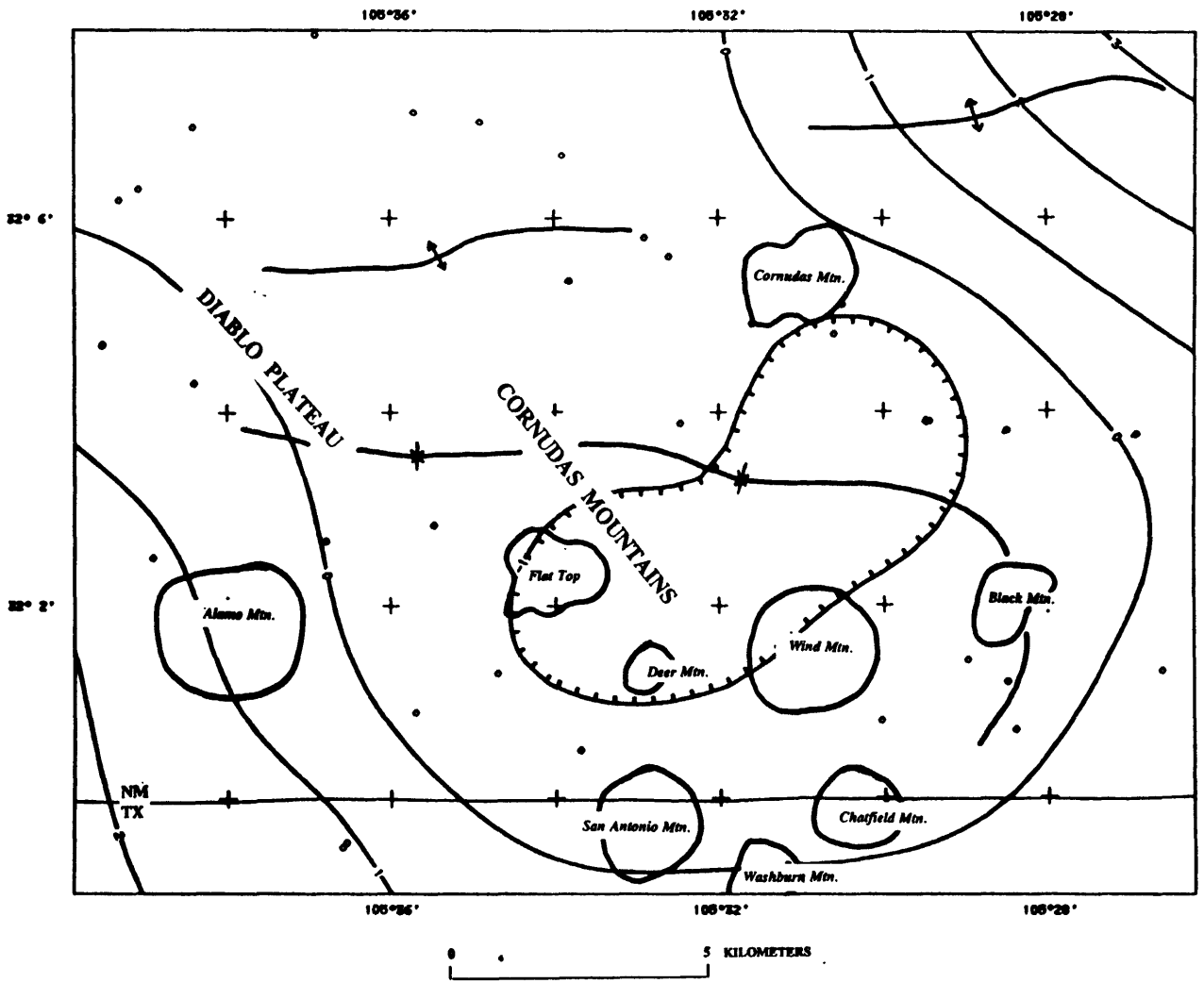

Figure 11. Residual gravity anomaly map of the Cornudas Mountains study area, southeastern Otero County, New Mexico, and northeastern Hudspeth County, Texas. Contour interval 1 milligal. Gravity control shown by small open circles; newly collected control by solid circles.

syncline that extends across the central part of the broad gravity low defined by the 0 mGal contour. Any correlation between the syncline and the deep source related to the residual gravity low is unknown. The anticlinal axes occur in the northern part of the map where there is some constriction of the residual gravity low (Fig 10b). The structural axes (Plate1) are plotted on the aeromagnetic map mainly for reference. The east-west trending anticlinal axes in the northern part of the area parallel east-west extensions of the aeromagnetic contours. The anticlinal axes are on either side of flight line control, but no geologic significance between the anticlinal axis and the parallel aeromagnetic contours can be inferred.

Electrical Resistivity Survey

Resistivity of rocks at low temperature is controlled to a large extent by water and clay content, both of which tend to lower resistivity from its normally high value in dry and unaltered rocks. Electrical resistivity information was acquired in the Cornudas Mountains area using the audio-magnetotelluric (AMT) geophysical method (Klein and Rodriguez, 1997). For these data, natural variations in the electric and magnetic fields at the surface of the earth were observed at 14 frequencies varying logarithmically from 4.5 to 27,000 Hz. Observations were made at 8 locations spaced at distances of 6.2 to 16 miles (11 to 26 km) apart to provide a reconnaissance of the subsurface resistivity in the area (Fig. 12). The interpreted data provide estimates of the distribution of the earth's resistivity to depths of about 1.2 mi (2 km).

Intrusions of the Cornudas Mountains are predominantly unaltered and are associated with highs in the magnetic field. Unaltered intrusions usually show high resistivity compared to shale or other clay-bearing sedimentary rocks. One goal of this study was to see if such high resistivity can be detected and if so, is it preferentially associated with rocks beneath magnetic highs. Such combined evidence could point to shallow, hidden intrusions beneath the surface. Also, the igneous rocks have deformed host rocks during intrusion (Plate1). Change in rock structure may have a signature in electrical resistivity because of the opening of rock fractures and the presence of small amounts of pore water and clay in the fractures.

Sounding locations (Fig. 12) were in part guided by aeromagnetic anomalies of igneous rocks. Wind Mountain, for example, is centered on an aeromagnetic high of about 300 nT (nanotesla, 1nT = 1 gamma) amplitude. Other aeromagnetic anomalies in the area not associated with known intrusive rocks may also indicate additional, buried intrusions. Observations were not limited to aeromagnetic highs, inasmuch as the object of the survey was to establish a broad areal resistivity signature. Some observations were placed off of the aeromagnetic highs to investigate background conditions in the subsurface. Table 1 and figure 13 summarize the results from AMT observations for each station. The estimated resistivity beneath each station is based on comparing theoretical data from various models to the observed data. The models used were composed of a sequence of 2 to 5 discrete horizontal layers; calculations of the theoretical data are based on algorithms similar to those described by Wait (1962) and Madden and Nelson (1985). The layer thickness and resistivities in the results of modeling are not uniquely or precisely established; error in a model amounting to 30 percent at a given depth and resistivity may be expected.

The results show no consistent correlation between the resistivity at depth and the aeromagnetic signature. Results from soundings in the western part of the study area indicate that at depths of less than 1.2 mi (2 km), the area is characterized by a profile from the surface downward of low/high/low resistivity. The thin upper low resistivity zone ranges in values typically from 5 to 50 ohm-m and has a maximum thickness of a few tens of meters. The second layer, with a thickness of a few hundred of meters, has a resistivity of 500 to 1,000 ohm-m or greater. The third layer has a resistivity of 1 to 500 ohm-m and cannot be distinguished below stations 2 and 4.

The resistivity picture outlined above is in accord with a thin, low-resistivity, altered and weathered top zone with generally high resistivity fresh rock below (2^{nd} layer). Layer 2 may represent relatively fresh Permian limestone and dolomite that underlies most of the Cornudas Mountains area (Plate 1); however, the high resistivity could also be represented by igneous intrusive rock such as sills intruded into flat lying carbonate rocks. The third layer, a low resistivity zone, may represent conductive clastic sedimentary rocks such as mudstone and shale. An interpretative geologic cross section across this area (Black, 1975) shows the Permian carbonate rocks exposed in the Cornudas Mountains to be underlain by shale, sandstone, conglomerate as well as thinly layered limestone of Pennsylvanian to Cambrian age.

Two profiles showing the resistivity determinations at depth are shown in Figure 13. Station spacing was too great to interpret detailed resistivity variations confidently between stations or to infer structural configuration in the subsurface; however, some broad features of the subsurface can be inferred. In the western part of the Cornudas Mountains, the thickness of the carbonate rocks that comprise layer 2

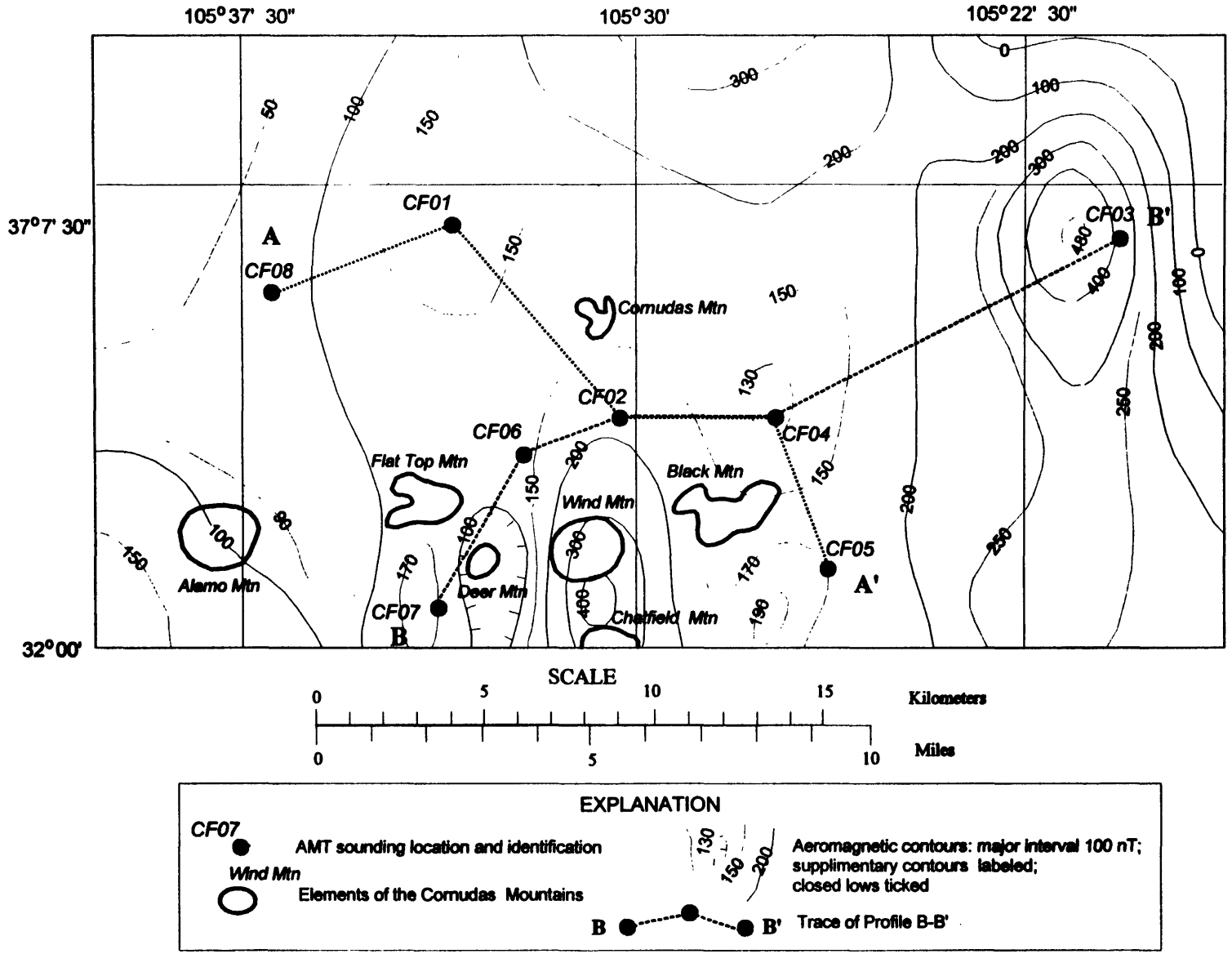

Figure 12. Location of AMT sounding stations (CF01 to CF08) in the Cornudas Mountains area, southern New Mexico. Contours show aeromagnetic anomaly values from a preliminary unpublished compilation (Dean Kleinkopf, USGS, Denver, April, 1996; data from Cordell, 1983).

Table 1. Summary of AMT soundings in the Cornudas Mountains area. The thickness of the deepest layer in all case is indefinite. The data quality column provides a subjective qualifier, based on scatter and how well a layered resistivity model fits the data. Resistivity values greater than 10,000 Ohm-m are questionable, but indicate high resistivity.

STA.	DATA QUALITY	LAYER RESISTIVITY (Ohm-m)	LAYER THICKNESS (m)	REMARKS
CF01	good	15 1000 30	10 400	On a broad 30 nT aeromagnetic high
CF02	very poor	15 200,000	10	On the north end of the Wind Mountain aeromagnetic high
CF03	poor	500 50,000 500 500,000	50 2,000 200	On flank of 1000 nT aeromagnetic high; broad topographic high
CF04	poor	20 10,000	20	On broad 20 nT aeromagnetic low; minor topography
CF05	good	20 1000 10 1000	3 200 50	On flank of 30 nT aeromagnetic low; minor topography
CF06	fair	50 1,000 10	20 100	On northwest flank of Wind Mountain aeromagnetic high
CF07	fair	10 1000 3	10 100	On 30 nT aeromagnetic high southwest of Deer Mountain
CF08	fair	10 1,000 1 30	5 200 30	On plains west of topography and aeromagnetic anomalies

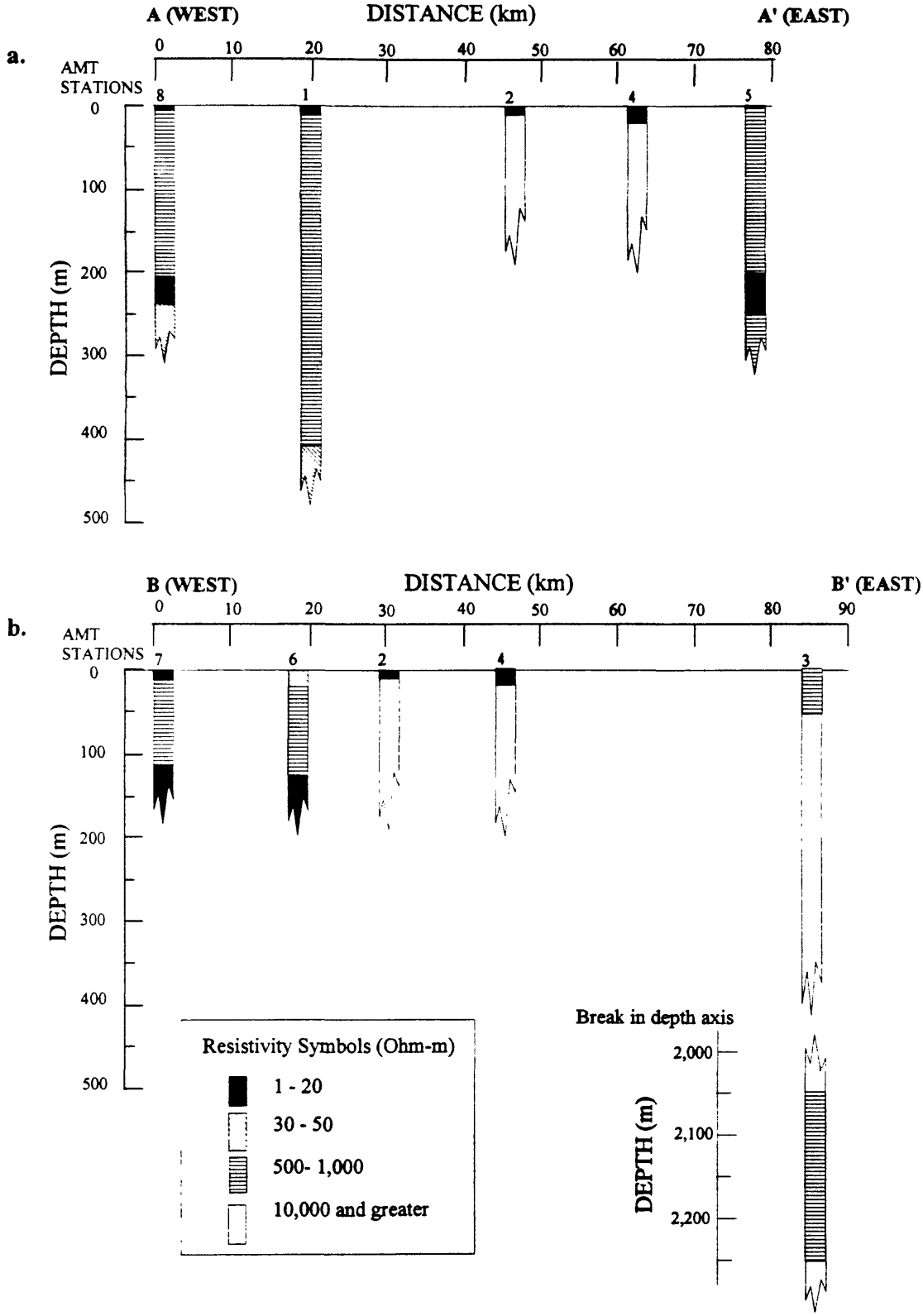

Figure 13. Resistivity versus depth profiles for AMT soundings in the Cornudas Mountains area, southern New Mexico. Stations are graphed as: **a.** profiles A-A' and **b.** profile B-B'; profile locations are shown on Figure 12. Soundings 2 and 4 are common to both profiles. Depth and resistivity parameters are listed in Table 1.

thicken from about 328 feet (100 meters) at stations 6 and 7, profile B-B' to about 492 feet (200 meters) to the northwest at station 8, profile A-A'. This thickening is probably a reflection of folding in this area; soundings taken at stations 6 and 7 are located in rocks assigned to the Hueco Formation, the oldest formation exposed in the area (Plate 1). Station 8 is located in the San Andres Formation that overlies the Hueco. Depth to conductive layer 3 would necessarily be greater at station 8 if the layer 3 truly represents clastic rocks below the Hueco. The data also show a structural break between stations 8 and 1, profile A-A'. Station 1 is located near the axis of an anticline that is clearly an extension of upwarping associated with the intrusion of igneous rocks at Cornudas Mountain, to the east (Plate 1). Increase in thickness of the resistive layer at station 1 probably represents the subsurface expression and westward extension of the Cornudas Mountain quartz-bearing syenite into the Hueco Limestone.

In the central part of the study area, soundings at 2 and 4 suggest that the third, conductive layer is missing and that layer 2 increases in resistivity and thickness. Intrusion of igneous rocks into layer 2 is a means to increase its resistivity as well as thickness. All stations are located on or near structural flexures mapped in the San Andres and Hueco formations—flexures that are associated with the intrusion of exposed igneous rocks (Plate 1).

On the east, both stations 3 and 5 are unique because they indicate a highly resistive fourth layer beneath the tripartite zonation detected on the west. Without additional soundings in this area, the significance of the results from soundings at stations 3 and 5 is vague. It is noteworthy, however, that an exploratory oil well, spuded in Permian rocks 10 miles (16 km) east of the Cornudas Mountains, penetrated Precambrian basement rocks directly beneath the Permian section (Black, 1975; King and Harder, 1985). Gravity data (this report), structure contours drawn on basement rocks in this area (Woodward and others, 1975), and interpretations of subsurface geology by Black (1975) indicate that the Cornudas Mountains lie just west of elevated basement rocks of the Pennsylvanian Pedernal uplift. It is likely that the highly resistive layer 4 detected at stations 3 and 5 reflects this abrupt change in subsurface lithology and structure.

ENVIRONMENTAL GEOCHEMISTRY

The study area lies within the northern Chihuahuan desert. The climate is semi-arid with hot dry summers and mild winters. Average annual precipitation (Fig. 14) varies from 12-14 inches (30-35 cm), with most precipitation occurring as thunderstorms during July and August (Mayer, 1995). Vegetation is mostly mixed desert scrub and desert grassland. No perennial surface water is present; therefore, all water resources are from the subsurface and its quality is an important issue. Regional ground water flow, based on contours on the water table (Fig. 15), is south and east toward the Salt Basin (Mayer, 1995). Ground water is pumped from wells and used mostly to water livestock. Because of the importance of ground water quality, the determination of the ground water chemistry and the processes responsible for the controls on the mobility and attenuation of elements in the ground water is the focus of this study. In addition, potential environmental geochemical impact that may result in future development, particularly mining, is discussed.

The area has been prospected for a variety of metals, but to date, no production has occurred (Schreiner, 1994; McLemore and Guilinger, 1993). Deposits of gold and silver are associated with alkaline igneous rocks in New Mexico (North and McLemore, 1988), but have not been found in economic concentrations in igneous rocks of the study area. Because no mining, milling, or smelting has taken place within the study area, no solid materials associated with mining are present. Therefore no samples of solid material were collected as part of the environmental geochemical investigation. Analytical methods, theoretical geochemical constraints, and chemical modeling and processes of well waters are discussed in detail by Miller (1997).

Aqueous Geochemistry

Waters were collected from 10 wells within the study area during April 25-26, 1996. Generally, wells were pumping prior to arrival at the site; if not, they were allowed to pump for 15 minutes before collecting the sample. Temperature, pH, and conductivity were measured at the site. In the laboratory, the remaining geochemistry was determined using various accepted analytical methods (see Miller, 1997).

The chemical analyses for the 10 filtered well water samples (Fig. 16) are shown in Table 2 . The ground waters are high in dissolved solids. Conductivity ranges from 866 to 3600 uS/cm. The pH values range from 6.60 to 8.28. The well waters are fresh to slightly saline and classified according to the dominant cation and anion. Eight of the ten wells are Ca^{2+}- SO_4^{2+} dominant waters, U47 is a Na^{+}- SO_4^{2+}

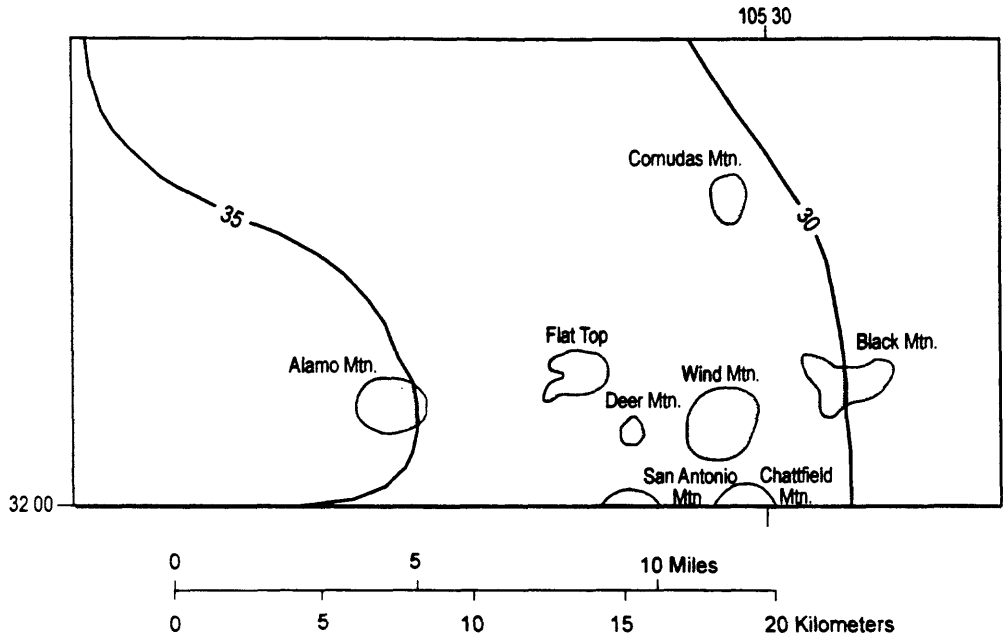

Figure 14. Map showing annual precipitation in centimeters for the Cornudas Mountains area (after Mayer, 1995)

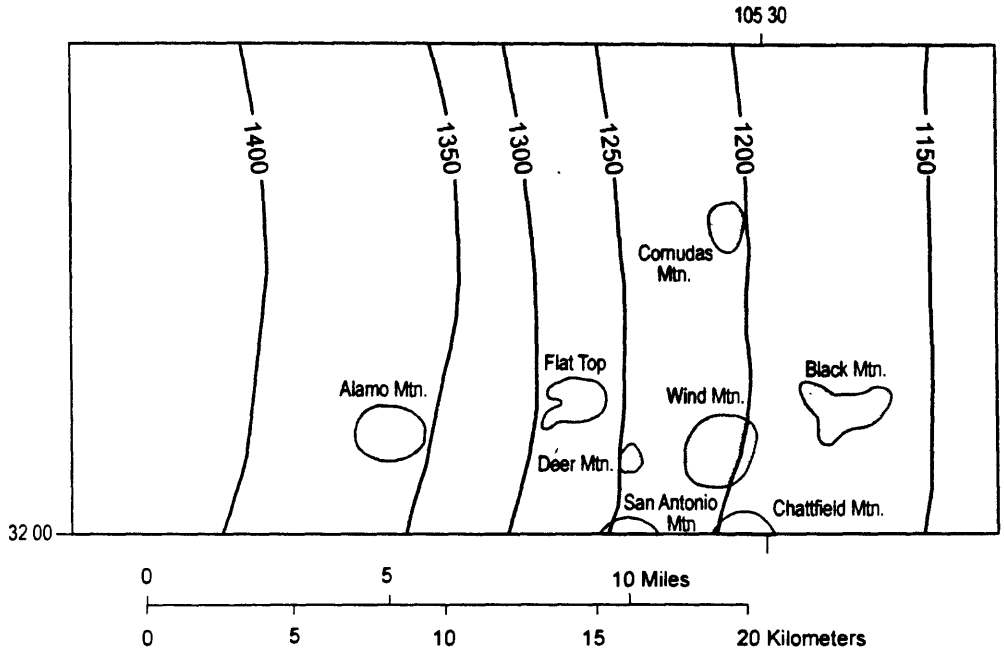

Figure 15. Potentiomentic surface elevations in meters above sea level in the Cornudas Mountains area (after Mayer, 1995).

Table 2. Chemical analyses of filtered well waters collected in the Cornudas Mountains, New Mexico

Site No.	Comments	pH	Conductivity uS/cm	Temperature Centigrade	Ca ppm	Mg ppm	Na ppm	K ppm
U38	well	7.21	2360	20.3	370	123	78	4.1
U39	Martin Lewis well	7.25	2390	20.8	420	131	40	2.8
U41	well	6.79	2710	22	530	122	74	4.9
U42	well	6.95	1287	21.5	150	56	70	3.1
U43	well	7.03	866	24.3	74	69	18	0.4
U44	well	6.6	2290	23.4	310	111	120	4.7
U45	Chess well	6.54	1785	20.1	250	88	64	3.5
U46	Pate well	7.15	1241	17.4	145	54	62	3.4
U47	Alamo well	8.01	3600	19	280	116	500	10
U48	Partnership well	8.28	2740	21	130	88	430	9.1

dominant water and U43 is a Ca^{2+}, Mg^{2+}- HCO_3^- dominant water. Well site U43 has the freshest water, but contains the highest NO_2 - NO_3 concentration at 7.6 ppm.

The concentrations of the heavy metals in the well waters vary considerably. The highest concentrations of iron occur at sites U38, U39, and U41 with values of 6200, 6580, and 4130 ppb respectively The source of some of the Fe is the pump, pipes and rods, but the dissolution of Fe-bearing minerals in the subsurface must also be taking place. Much lower in concentrations and less variable are Mn and Al. Of the base metals, only Zn, Cu, and Mo occur in anomalous concentrations above normal background abundances expected in this geologic setting, with values of Zn up to 450 ppb, Cu up to 20 ppb, and Mo up to 90 ppb (Table 2). When water is pumped from the wells, the water comes into contact with metal pumps, pipes, and rods, which is probably the source for the anomalous values of Fe, Zn, Cu, and Mo in the well water. Other trace elements are generally at background concentrations of less than 1 ppb.

In addition to this study, wells within the study area have been sampled for chemical analyses previously. Eleven wells within the study area (Fig. 16a) were sampled in 1976 during the U.S. Department of Energy's National Uranium Resource Evaluation (NURE) program. Geochemical data for well waters collected during this program were obtained from Hoffman and Buttleman (1994). In addition, in 1992, Mayer (1995) sampled 15 wells within the study area (Fig. 16c).

The combined geochemical studies in this area represent three different ground water geochemistry baselines that can be compared to determine changes in the chemistry with time. Chemical analyses of ground waters from the two prior studies are shown in Tables 3 and 4. A comparison of ground water chemistry of specific well sites collected during the three different time periods can be made (Table 5). The most significant trend between 1974 and 1996 is that conductivity increased (Table 6). The Alamo well had the greatest increase in conductivity (106%). For this site, the major elements, calcium and sodium had significant increases during this time period (233% and 56%). The remaining elements and pH did not vary significantly during this time period. At the other sites, none of the species or pH varied significantly during this time period.

High concentrations of nitrate were found by Mayer (1995). The comparisons of nitrate from Mayer (1995) and total $NO_2 + NO_3$ concentrations in well waters analyzed in this study are shown in Table 7. There is significant difference in the two sets of data that is difficult to explain. If Mayer's (1995) values are correct, then the high values may be due to leaching of cattle waste during runoff after storms and leaking of nitrate into the ground water in the vicinity of the well, accounting for the high values.

The oxidation potential (Eh) ranged from 0.264 to -0.034 volts (Table 8). The most oxidizing conditions are sites U44 and U45 which are both located along Chess Draw north of Wind Mountain. The most reducing conditions are sites U47 and U48, which are both located north of Alamo Mountain.

Chemical Models and Processes

To gain understanding of processes such as speciation of elements, redox conditions, and identification of minerals that may control the mobility, attenuation, and concentrations of elements in the waters, chemical modeling of the well waters using saturation indexes have been calculated by Miller (1997). The indexes indicate that mineral phases may be controlling concentrations of elements in the well waters. The source of the water in the study area is precipitation which falls within the immediate area. The chemical composition of the water is derived from the composition of the bedrock. In addition, wind-born dust picked up within the study area or from outside the study area can be deposited as aeolian material within the study area. Waters, coming into contact with this material, can pick up additional constituents.

The results (Table 8) indicate that for many of the well waters, gypsum, calcite, dolomite, and chalcedony are near saturation, saturated or supersaturated with respect to the well waters, indicating that these phases play a major role in controlling the concentrations in the well waters [see Miller (1997) for details on interpretation of saturation indexes]. All of the waters are near saturation, saturated or supersaturated with respect to calcite and chalcedony, four of the well waters are saturated with respect to gypsum, seven of the well waters are saturated or supersaturated with respect to dolomite, and seven of the well waters are saturated with respect to fluorite.

The dissolution of gypsum is responsible for the high concentrations of Ca^{2+} and SO_4^{2-} in many of the well waters within the study area. Every well sampled in this study, with the exception of U44, was drilled in the gypsiferous Permian San Andres Formation and probably penetrated the underlying, gypsum-rich Yeso Formation (Plate 1). Well U44 was drilled in the Permian Hueco Limestone that does not contain

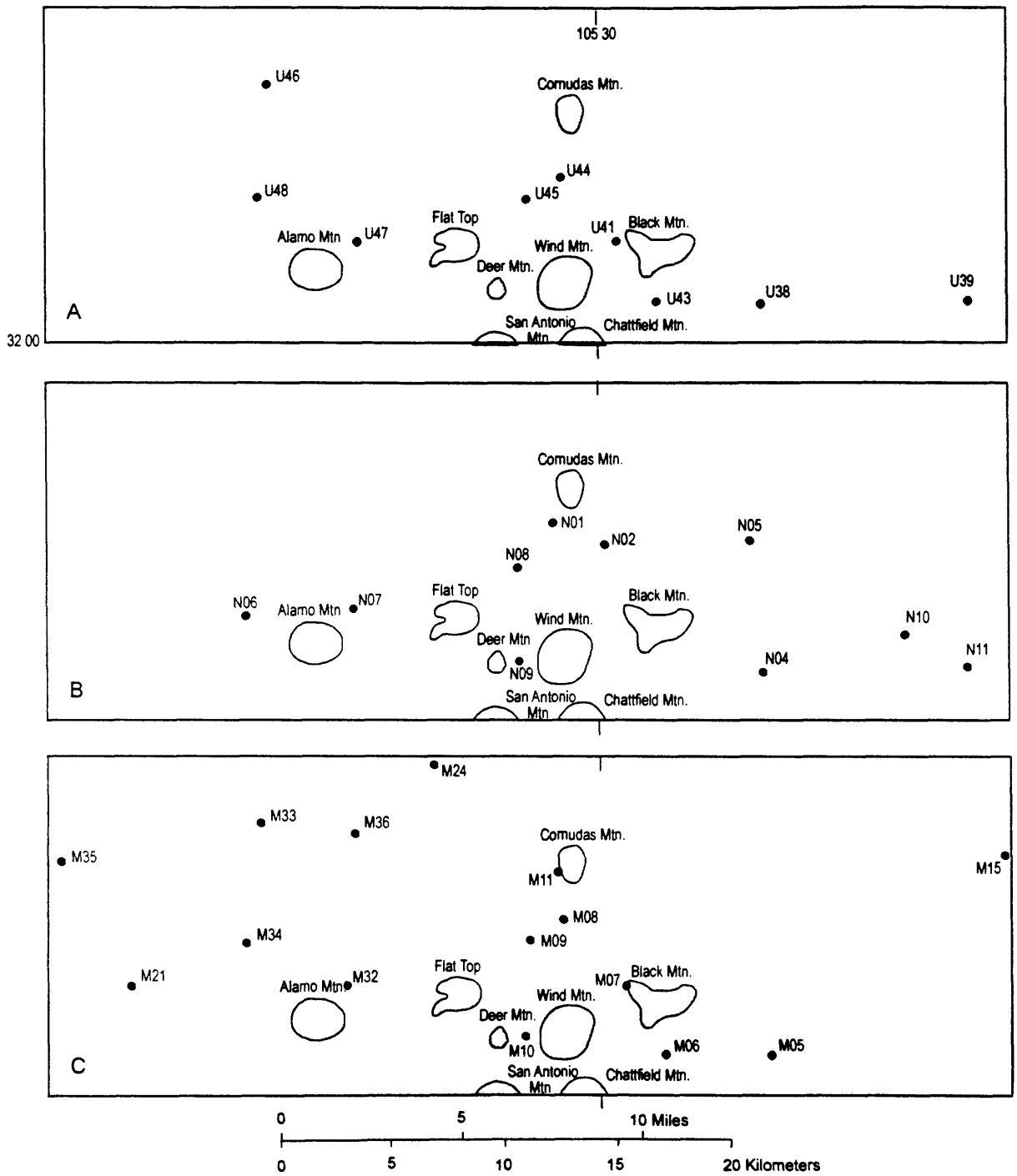

Figure 16a. Map showing locations of wells sampled in the Cornudas Mountains area for this study.

Figure 16b. Map showing locations of wells sampled during the NURE program in the Cornudas Mountains area.

Figure 16c. Map showing locations of wells sampled by Mayer (1995) in the Cornudas Mountains area.

Table 3. Chemical analyses of well waters collected during the NURE program in mid 1970's, from Hoffman and Buttleman (1994)

Site	Temp. deg C	pH	Cond. µS/cm	Al ppb	B ppb	Ba ppb	Ca ppm	Cr ppb	Cu ppb	Fe ppb	K ppm	Li ppb
N01	26	6.90	1600	101	635	7	309	<4	15	43	5.9	115
N02	25	7.10	155	282	23	62	37	12	5	332	4.8	4
N03	21	6.90	780	95	154	98	73	<4	5	84	0.3	9
N04	20	6.90	1650	112	516	13	415	<4	10	624	4.6	139
N05	26	7.10	1825	67	510	23	650	<4	5	77	7.1	116
N06	25	6.30	2100	38	1405	11	121	<4	9	34	6.3	82
N07	26	8.00	1750	338	1732	16	84	18	10	162	9.4	178
N08	24	6.50	1300	16	439	14	247	<4	3	48	3.1	76
N09	19	7.10	550	19	124	42	62	<4	12	23	4.7	10
N10	25	7.60	1300	150	749	28	913	<4	15	110	7.5	136
N11	20	7.40	2200	24	306	12	428	<4	5	296	2.7	57

Mg ppm	Mn ppb	Mo ppb	Na ppb	Nb ppb	Ni ppb	P ppb	Sr ppm	Zn ppb
131	6	16	101	14	<4	<40	10.6	108
2	131	15	2	<4	<4	146	0.1	31
66	18	4	25	<4	<4	<40	1.2	229
138	54	25	87	10	23	<40	12.0	11018
165	21	12	56	<4	<4	<40	16.7	892
61	9	95	467	<4	21	<40	4.9	68
92	9	16	320	13	39	<40	6.6	82
85	19	24	62	<4	<4	<40	7.3	239
33	27	169	37	14	<4	<40	4.4	1229
279	25	9	96	35	6	56	23.6	239
124	21	15	44	19	14	<40	10.1	164

Table 3. Chemical analyses of well waters

Fe ppb	Co ppb	Ni ppb	As ppb	Se ppb	Br ppb	Mo ppb	U ppb	Pb ppb
6200	1.6	14	0.3	1.5	410	20	9	0.5
6580	1.2	7	<.2	1.9	210	8	4	0.6
4130	1.2	3	1.3	1	350	36	<.02	0.6
179	0.3	2	1.6	11	300	28	16	0.6
133	0.7	9	0.4	2.4	150	5	14	0.6
87	0.5	5	0.5	14	920	26	19	0.5
178	0.5	4	<.2	15	410	21	15	0.6
103	0.8	5	0.4	21	400	21	<.02	0.5
90	0.5	<.02	0.6	5.7	1540	32	12	0.6
46	0.3	<.02	0.3	3	1580	90	8	0.6

SiO2 ppm	Alkalinity ppm	Sulfate ppm	Cl ppm	F ppm	NO2+NO3 ppm	Cu ppb	Zn ppb	Li ppb	Al ppb	Cr ppb	Mn ppb
16	305	1400	50	1.9	<0.02	0.2	220	57	17	3	230
13	244	1500	32	1.4	<0.02	3	450	43	22	1	360
23	268	1700	46	2.2	<0.02	0.1	210	63	5	2	46
41	183	500	34	2.2	1.9	3	190	30	2	3	14
40	427	18	12	0.8	7.6	20	390	8	4	2	48
21	378	1000	110	2.3	2.6	4	29	58	11	5	7
24	380	780	48	2.2	2.1	5	120	50	16	2	8
24	285	470	36	2.3	nd	4	310	46	7	1	21
17	293	1900	170	3.3	nd	2	88	131	11	4	9
16	345	1100	170	4.6	nd	2	30	69	19	3	16

Table 4. Chemical analyses of filtered well waters from from the Cornudas Mountains area from Mayer (1995)

SITE	TEMP deg C	pH	COND uS/cm	HCO3 ppm	Na ppm	K ppm	Mg ppm	Ca ppm	Cl ppm	NO3 ppm	SO4 ppm
M05	20	7.1	2500	229	84	8.3	123	334	45	7.2	1120
M06	18.6	7.15	700	564	15	—	70	71	11	29	15
M07	19.8	6.98	2950	243	80	8.7	129	466	37	0.1	1490
M08	19.3	6.95	2300	337	141	8	115	273	118	10	933
M09	18.6	7.1	1600	359	58	8.1	84	220	40	9.8	655
M10	20	7.66	700	293	35	9	32	58	18	4.4	81
M11	—	7.4	200	52	5.5	1.3	3	27	1.8	17	19
M15	23.9	6.98	2500	166	56	5.9	126	346	11	0.1	1410
M21	20.7	6.91	3500	400	233	11	130	342	86	1.6	1360
M24	15.2	7.37	1200	361	50	6.3	74	70	56	30	173
M32	19.7	7.1	3450	340	421	9.6	92	257	118	0.1	1320
M33	16.5	6.81	3000	289	61	8	52	136	28	24	396
M34	18.6	7.26	3000	420	361	8.9	65	114	191	0.1	798
M35	17.5	6.81	3300	467	84	12	139	441	47	5.7	1470
M36	18.6	6.9	4350	426	375	34	167	340	238	0.7	1730

Table 5. Comparison of selected chemical analysis for a specific site collected in 1974, 1992, and 1996

	TIME	SITE	pH	COND uS/cm	Ca ppm	Mg ppm	Na ppm	K ppm
Unnamed	1974	N04	6.9	1650	415	138	87	4.6
well #1	1992	M05	7.1	2500	334	123	84	8.3
	1996	U38	7.21	2360	370	123	78	4.1
Unnamed	1974	N03	6.9	780	73	66	25	0.3
well #2	1992	M06	7.15	700	71	70	15	--
	1996	U43	7.03	866	74	69	18	0.4
Chess	1974	N08	6.5	1300	247	85	62	3.1
well	1992	M09	7.1	1600	220	84	58	8.1
	1996	U45	6.54	1785	250	88	64	3.5
Alamo	1974	N07	8	1750	84	92	320	9.4
well	1992	M32	7.1	3450	257	92	421	9.6
	1996	U47	8.01	3600	280	116	500	10

Table 6. Comparisions of conductivity at four well sites for waters collected in 1974 and 1996

SITE	COND uS/cm 1974	COND uS/cm 1996	DIFFERENCE percent
well #1	1650	2360	43
well #2	780	866	11
Chess well	1300	1785	37
Alamo well	1750	3600	106

gypsum-bearing interbeds. Several of the well waters are undersaturated with respect to gypsum. This undersaturation may be due to the nonuniform occurrence of gypsum in the subsurface.

High concentrations of elements associated with chalcedony, calcite, and dolomite in well water is due to the fact that all rocks encountered in each well carry abundant chert nodules and stringers, and generally vary only slightly in their limestone and dolomite content (Plate 1). Wells U47 and U48 were drilled in the stratigraphically highest rocks of the San Andres Formation which is much less dolomitic than strata lower in the formation.

The elevated chloride contents of the ground water is probably due to the dissolution of halite associated with evaporite layers of the Yeso Formation. The presence of both gypsum and halite in ground water reservoirs will yield high contents of Ca, Na, and SO_4^-

Ground water in contact with carbonate minerals, which are abundant in the bedrock of the study area (Plate 1), should be buffered to a pH value of approximately 8.2. The pH values of the well waters are lower and are slightly acid to slightly alkaline, indicating that other processes are responsible for the lower pH. One process active in the study area is dedolomitization which lowers pH by increasing the concentration of Ca into the well waters through the dissolution of gypsum (see Miller, 1997, for details). A second contributing process may involve the oxidation of sporadic petroleum and organic material that may be present in the sedimentary rocks. This will oxidize and use up the oxygen in the ground water causing a decrease in the oxidation potential. A third process which may be responsible for lowering pH is that some of the sulfate which is abundant in the ground waters may be reduced to HS^- or H_2S by the reducing environment. The process will generate acid which will lower the pH of the ground waters. The reducing environment and acid pH values will also cause the release of iron and manganese to the ground waters. The net effect is well water with a pH of around 7 or slightly less instead of an alkaline value of 8.2. In addition, this slightly acidic and reducing solution will react with the casings, pump rods, and pipes, releasing elevated concentrations of iron, manganese, zinc, and copper to the ground waters and requiring the rods to be replaced sooner than normal.

Discussion

Natural and anthropogenic-related sources can contribute heavy metals and acid to the environment. The purpose of this section is to identify environmental problems that may presently exist or potentially exist if mining occurs within the study area in the future. The study area is sparsely populated, no industry is present, and no mining has taken place. There is no evidence, such as anomalous concentrations of metals in the ground water, that the large smelter in El Paso has any effect in the study area. Therefore, environmental concerns must be considered in the context of local geology and in particular, the composition of the rocks. Any present geochemical environmental problems are the result of natural processes that occur when the rocks of the study area are subjected to chemical and mechanical weathering. Pyrite is the main mineral, that when oxidized, will have the greatest effect of releasing acid and heavy metals to the natural waters of an area. Pyrite is mostly absent from the study area. In addition, the chemical composition of rocks present in the area, namely limestone and dolomite, gypsum-bearing sandstone and shale, and alkaline igneous rocks, generally contain normal low concentrations of trace elements such as Zn, Cu, Pb, Cd, and Hg. Other trace elements in the rocks, such as As, are also probably low. Consequently there is minimal amounts of heavy metals and acid released from the rocks to the waters during normal weathering.

Two lithologies present in the study area are effective for mitigating any acid drainage that may presently or in the future be generated: 1) limestones and dolomites and 2) caliche that is abundant as cement in alluvium. The carbonate minerals react with the waters, buffer the H^+, and raise the pH. Heavy metals such as Cu and Zn, if present, will hydrolyze and precipitate at the higher pH values.

The other major rock group in the study area are the alkaline intrusions. These rocks have limited buffering capacity, mainly from minerals such as plagioclase. But the ubiquitous occurrence of calcite in the surficial material and sedimentary rocks surrounding these intrusions will provide buffering capacity to neutralize any acid generated in the surface.

Climate plays a significant role in geochemical processes. Water is necessary for chemical weathering to occur. The climate of the study area is semi-arid. Because of the low annual precipitation, chemical weathering at the surface probably takes place in pulses when water is present following runoff from storms. In contrast to the surface, within the zone of ground water, water is in continuous contact with the rocks and chemical processes are continuously taking place.

Table 7. Comparisons of concentrations of nitrate (from Mayer,1995 with nitrite + nitrate (this study)

STUDY	SITE	CONCENTRATION
Mayer (1995)	M05	7.3 ppm nitrate
This study	U38	<0.02 ppm nitrite + nitrate
Mayer (1995)	M06	29 ppm nitrate
This study	U43	7.6 ppm nitrite + nitrate
Mayer (1995)	M09	9.8 ppm nitrate
This study	U45	2.1 ppm nitrite + nitrate
Mayer (1995)	M08	10 ppm nitrate
This study	U44	2.6 ppm nitrite + nitrate

Table 8. Saturation index values of four minerals for well waters, Cornudas Mountains, New Mexico

SITE	Eh (v)	GYPSUM	CALCITE	DOLOMITE	CHALCEDONY	FLUORITE
U38	0.051	-0.26	0.37	0.54	0.04	-0.14
U39	0.042	-0.2	0.36	0.5	-0.06	-0.37
U41	0.134	-0.09	0.04	-0.26	0.18	0.07
U42	0.179	-0.85	-0.32	-0.77	0.43	-0.2
U43	0.169	-2.45	-0.01	0.29	0.38	-1.31
U44	0.264	-0.44	-0.14	-0.4	0.12	-0.05
U45	0.259	-0.56	-0.29	-0.75	0.22	-0.08
U46	0.165	-0.88	0	-0.19	0.25	-0.12
U47	-0.034	-0.33	0.92	1.73	0.08	0.16
U48	-0.007	-0.76	1.04	2.2	0.02	0.2

The geochemical environmental consequences of future mining would have minimal impact on the water chemistry. Nepheline syenite in the Cornudas Mountains, if mined, has a limited buffering capacity and contains little or no pyrite or other sulfide minerals that generate acid and degrade the water. Possible dewatering of the aquifer for mining use is not considered.

Conclusions

Within the surface environment, runoff from precipitation will quickly acquire Ca^{2+} and SO_4^{2-} from the dissolution of abundant gypsum present in the Permian Yeso Formation and/or gypsiferous wind blown dust. In addition, the abundant carbonate minerals will buffer the ephemeral surface waters to pH of approximately 8.2. Other processes affect the waters in the subsurface. Additional Ca^{2+} and SO_4^{2-} can be picked up by the ground water from the dissolution of gypsum within the sedimentary rocks as well as Na^+ and Cl^- from halite. Dedolomitization causes the increase of Ca^{2+}, Mg^{2+}, and SO_4^{2-}, a decrease in pH, and a slight decrease in bicarbonate concentration. Although carbonate minerals are common in the subsurface, the presence of organic material and possibly petroleum in the aquifer uses up the oxygen causing a reducing environment. Some of the sulfate is reduced to HS^- or H_2S, causing the pH to change from 8.3 to neutral to slightly acid. This water will dissolve metals such as iron, manganese, zinc, and copper from the well casing, rods, and pipes. These elevated concentrations of metals, if released to the surface material, will quickly be reduced in metals and acid by buffering by carbonate minerals and therefore are of little consequences (except for more frequent replacement of well parts) in terms of the geochemical environmental problems. The presence of cattle, particularly around the wells, may lead to an elevated concentrations of nitrate due to leaking of nitrate from cattle waste into the ground water in the vicinity of the well during storm runoff.

In summary, the main geochemical environmental concern presently in the study area is: (1) the presence of slightly saline water due to the abundant gypsum and sometimes halite; (2) the neutral to slightly acid ground waters due to dedolomitization or reduction of sulfate; and (3) the elevated concentrations of nitrate, possibly due to leaching of cattle wastes in the vicinity of well sites. These problems, except for the nitrate, are due to natural processes that have operated for at least 1000's of years. Possible future mining would probably have no significant impact on the chemistry of the surface or ground waters.

MINERAL RESOURCES

Appraisal of Identified Resources

The Cornudas Mountains were historically explored for deposits associated with alkaline igneous rocks--uranium, beryllium, rare-earth elements, niobium, and gold and silver--and industrial minerals (McLemore and Guilinger, 1993; Schreiner, 1994), but there was no production except for test shipments of nepheline syenite for use as sand-blasting material in 1995. More recently (1991-1995) Addwest Minerals, Inc. explored the Wind Mountain nepheline syenite for use in manufacturing amber-colored beverage containers, flatware, and ceramics and for use as an abrasive and as roofing granules (McLemore and others, 1996a). Several small test shipments of nepheline syenite were sent for testing for use as sand blasting material. In response to the interest by Addwest Minerals, Inc, in 1992 the U.S. Bureau of Mines conducted a field investigation in the Wind Mountain and Chess Draw area; the study consisted of mapping and sampling of prospects and includes 35 chemical analyses (Schreiner, 1994). Table 9 summarizes known prospects in the Cornudas Mountains.

Uranium, beryllium, rare-earth elements, niobium, and gold and silver

In the 1950's uranium prospectors located several areas of anomalously high radioactivity and attributed it to the presence of uranium. Shallow prospect pits were dug on many of the claims in the area, but assay results were low and the claims were later dropped with no production (Table 9). In 1956, the U.S. Atomic Energy Commission examined the area to evaluate the potential for uranium (Collins, 1958) and recommended no further work. Uranium and thorium occur disseminated within the dikes and intrusions; samples range from 0 to 0.8% U_3O_8 (Collins, 1958) and from 13-351 ppm Th (Schreiner, 1994).

Beryllium was first reported from the Cornudas Mountains during the 1940s (Warner and others, 1959) and a few rock samples assayed as much as 0.2% BeO. Beryllium occurs in feldspar, nepheline, aegirine, and eudialite in igneous rocks in the Cornudas Mountains; no beryllium minerals have been identified.

Table 9—Mines and prospects in the Cornudas Mountains, Otero County, New Mexico

MINE NAME (ALIAS)	LOCATION	LATITUDE	LONGITUDE	COMMODITIES	DEVELOPMENT	REFERENCES
Chess Draw (Wind Mountain)	17, 18 26S 14E	32° 3' 15"	105° 31' 45"	U, Th, Be	pits, 15 ft, 12 ft shafts	Collins (1958), Warner and others (1959), Zapp (1941), McLemore (1983), Schreiner (1994)
Jones	S22 26S 14E	32° 1' 30"	105° 30' 5"	U, Th, Be	no workings	Holser (1959), Collins (1958), Zapp (1941), McLemore (1983)
Llewellyn	SW2 25S 14E	32° 4' 10"	105° 29' 25"	U, Th, Be, Nb	25 ft adit, caved (covered)	Collins (1958), Zapp (1941), McLemore (1983)
Wind Mountain	SE20 26S 14E	32° 1' 20"	105° 31' 45"	U, Th, Be, Pb, Zn	pits, 22 ft adit	McLemore (1983), Holser (1959), Schreiner (1994)
Wind Mountain nepheline syenite	28 26S 14E	32° 00' 56"	105° 31' 25"	nepheline syenite	150 ft adit	McLemore and others (1994, 1996a, b), McLemore and Guilinger (1993, 1996), Schreiner (1994)
Deer Mountain	19 26S 14E	32° 1' 20"	105° 31' 55"	nepheline syenite	none	McLemore and Guilinger (1993, 1996), Schreiner (1994)

Table 10—Selected minerals and their occurrence reported from the Cornudas Mountains. Chemical Formulae of Rare Species: [1]$Na_4(Ca, Ce)_2(Fe^{2+}, Mn^{2+})\ YZrSi_8O_{22}(OH,Cl)_2$; [2]$Na_2ZrSi_3O_9 \cdot 2H_2O$; [3]$NaKZrSi_3O_9 \cdot 2H_2O$; [4]$Na_2ZrSi_2O_7$

MINERAL	OCCURRENCE	REFERENCE
anaclime	replaces nepheline, lines vugs, vesicles and miarolitic cavities	Barker and Hodges (1977), Boggs (1985)
natrolite	replaces nepheline and feldspars	Barker and Hodges (1977)
olivine	mineral aggregates of ferromagnesian minerals and magnetite	Barker and Hodges (1977)
aenigmatite	in nepheline syenite	Barker and Hodges (1977)
eudialyte[1]	in dikes, sills, and laccoliths and in marolitic cavities	Barker and Hodges (1977), Clabaugh (1950), Boggs (1985, 1987)
catapleiite[2]	miarolitic cavities	Boggs (1985)
georgechaoite[3]	miarolitic cavities	Boggs (1985), Boggs and Ghose (1985)
aegirine (acmite)	miarolitic cavities	Boggs (1985, 1987)
monazite	miarolitic cavities	Boggs (1985)
thomosonite	miarolitic cavities	Zapp (1941), Boggs (1985)
chabazite	miarolitic cavities	Boggs (1985)
parakeldyshite[4]	nepheline syenite, Wind Mountain	McLemore (1996)
pyrite	mineral aggregates of ferromagnesian minerals	McLemore and others (1996a)
fluorite	breccia	Barker (1977)

In the Chess Draw area, northwest of Wind Mountain, only one rock sample contained 150 ppm Be whereas the remaining samples from that area contained less than 100 ppm Be (U. S. Borax, written communication, January 1986; Schreiner, 1994).

The abundant rare mineralogy of Wind Mountain (Table 10) has led to exploration for deposits of rare earth elements, niobium, and zirconium. In 1984, Leonard Minerals Co., in conjunction with U. S. Borax Corp., conducted an exploration program for rare-earth elements, niobium, and zirconium. Mapping, sampling, and drilling in the Chess Draw area failed to discover any significant mineralized zones (New Mexico Bureau of Mines and Mineral Resources files). Assays were low (up to 0.06% total rare-earth oxides, 10-1400 ppm Nb, 10-3000 ppm Zr, 230-13,000 ppm F). An analysis reported by McLemore and others (1988a, b) contained 1235 ppm Ce, 700 ppm La, 270 ppm Nd, and 242 ppm Y (sample #7368). Analyses reported by Schreiner (1994) are also low and subeconomic: as much as 3790 ppm total REE, 2332 ppm Nb, 92 ppm Be, and 3137 ppm F. Zirconium silicates are common in the area and assays as high as 9919 ppm Zr are reported (Schreiner, 1994, appendix A). The 1994 U.S. Bureau of Mines evaluation for rare earth and niobium resources in the Wind Mountain and Chess Draw area also concluded there was no resource (Schreiner, 1994).

Numerous private companies have examined the Cornudas Mountains for gold-silver deposits related to the Tertiary alkaline intrusive rocks, but without success (McLemore and Guilinger, 1993). U. S. Borax sampled and drilled in the Chess Draw area, but their samples contained only trace amounts of gold and silver. For the U.S. Bureau of Mines study, Schreiner (1994, appendix A) collected and assayed 35 rock samples, which ranged from <5 to 20 ppb Au and <0.2 to 5.2 ppm Ag (Table 11). McLemore and Guilinger (1993) analyzed four altered rock samples in the Chess Draw area: one sample contained a trace of gold (<0.02 oz/ton) and 0.78 oz/ton Ag).

Industrial minerals

Nepheline syenite is a constituent in manufacturing glass, ceramics, and flatware (Allen and Charsley, 1968; Guillet, 1994; Bourne, 1994; O'Driscoll, 1990; Potter, 1990). Nepheline syenite is an inexpensive source of essential alumina, soda, and ash.; improves the workability of the glass batch by lowering the viscosity; and imparts a unique quality of toughness to the glass which makes it more resistant to breakage. In addition, nepheline syenite is used as extender pigments, fillers, roofing granules, dimension stone, abrasive, and aggregate (Allen and Charsley, 1968; Guillet, 1994; McLemore and Guilinger, 1993, 1996; McLemore and others, 1994, 1996a). Nepheline syenite is desired in pigments and fillers because it has a high brightness, inertness, and easy wetting and dispersion in parent formulations. The UV attenuation characteristics and resistance to weathering of nepheline syenite provide for use as roofing granules by blocking sunlight and from degrading in asphalt roof. The lack of quartz or free silica and relative hardness also enables use of nepheline syenite as a silica-free abrasive. Nepheline syenites have also been examined for potential sources of alumina and alkalis (Allen and Charsley, 1968). Other potential uses include as fertilizers, ingredients in refractory cement, and paper (Allen and Charsley, 1968).

The outer zone of the Wind Mountain nepheline syenite was explored by Addwest, Inc., for use as a constituent in glass, ceramics, and flatware and for use as an abrasive. The nepheline syenite contains high iron (Table 12) compared to other commercial sources of nepheline syenite. However, when the Wind Mountain nepheline syenite is crushed and passed through a specialized rare-earth magnet, the resulting product is similar in composition to Grade B product specified by Unimin Canada Ltd. (Table 13) and has been certified by Coors Inc. as being suitable for amber-colored glass and ceramics. The lack of free silica, i.e. no quartz, and a Mho's hardness of greater than 6 enables use of the Wind Mountain nepheline syenite as a silica-free abrasive (McLemore and others 1994, 1996a, b; McLemore and Guilinger, 1996). Physical and chemical test results of Wind Mountain nepheline syenite meet or exceed standards for use as roofing granules, dimension stone, aggregate, and abrasives (McLemore and Guilinger, 1996).

Mining proposed by Addwest Minerals was by underground, room and pillar methods. Processing would involve crushing, grinding, magnetic separation, and screening. At full production, Addwest expected to process 3,000 short tons per day or 700,000 short tons per year. Current proven, probable, and inferred reserves total 200 million short tons for a mine life of more than 100 years (Industrial Minerals, 1995).

Assessment of Potential for Undiscovered Resources

This assessment considers uranium, beryllium, rare-earth elements, niobium, gold and silver, and nepheline syenite for industrial uses. The lack of sulfides in any rocks in the study area and the scarcity of

Table 11—Chemical analyses of rock samples from the Chess Draw area (McLemore and Guilinger, 1993; Schreiner, 1994).

SAMPLE NUMBER	LOCATION	Au (oz/ton)	Ag (oz/ton)	Cu (ppm)	Pb (ppm)	Zn (ppm)	Hg (ppm)
7368	18 T26S R14E	tr (<0.02)	0.78	—	—	—	—
CORN 16	18 T26S R14E	0.00	0.00	10	15	62	0.05
CORN 17	18 T26S R14E	0.00	0.00	122	195	122	0.17
CORN 19	18 T26S R14E	0.00	0.00	27	22	34	0.02
USBM 4	NE18 T26S R14E	0.0003	<0.006	9	6	43	0.02
USBM 19	SE20 T26S R14E	0.0005	0.15	30	118	278	0.02
USBM 20	SE20 T26S R14E	0.0006	0.05	23	185	732	<0.01
USBM 22	SE20 T26S R14E	<0.00001	0.15	42	86	114	<0.01

Table 12—Chemical composition of unprocessed, raw nepheline syenite from Cornudas Mountains, New Mexico and from Blue Mountain, French River, and Rutter, Ontario, Canada, which have been used for manufacturing glass. [1]From McLemore and Guilinger (1993) and McLemore et al. (1996a, b), unaltered surface and drill core samples (n=5). [2]Average from Barker (1977, n=4) and Schreiner (1994, n=2). [3]From Guillet (1994). * Total iron as Fe_2O_3.

	AVERAGE WIND MOUNTAIN ($TNSP_2$)[1]	RANGE OF WIND MOUNTAIN ($TNSP_2$) SAMPLES[1]	DEER MOUNTAIN[2]	BLUE MOUNTAIN, ONTARIO[3]	FRENCH RIVER, ONTARIO[3]	RUTTER, ONTARIO[3]
SiO_2	59.84	56.3 - 63.3	57.3	59.18	56.35	59.03
TiO_2	0.12	0.03 - 0.14	0.48	0.06	0.16	0.03
Al_2O_3	18.84	17.6 - 20.8	19.6	23.06	20.31	21.81
Fe_2O_3*	4.90	1.54 - 6.48	6.85	2.15	7.19	3.82
MgO	0.73	0.07 - 1.80	0.44	0.17	0.11	0.06
CaO	1.23	0.68 - 1.40	1.52	0.76	1.69	0.53
K_2O	5.35	4.80 - 6.32	5.46	3.94	4.86	4.36
Na_2O	7.82	7.20 - 8.80	7.03	10.48	8.31	10.78
MnO	0.27	0.14 - 0.35	0.38	—	0.18	0.03
P_2O_5	0.11	<0.05 - 0.11	0.13	0.02	0.04	0.02
LOI	2.24	1.02 - 2.91	2.62	0.40	1.36	0.15
TOTAL	101.45	—	101.81	100.22	100.56	100.62

Table 13—Chemical analyses of nepheline syenite after magnetic separation from Wind Mountain, New Mexico compared to raw composition of typical glass grade compositions of Blue Mountain and Elkenm Neflin nepheline syenites. *Total Iron as Fe_2O_3.

	WIND MOUNTAIN $TNSP_2$ PIT 1	WIND MOUNTAIN $TNSP_2$ PIT 2	UNIMIN CANADA LTD. A GRADE	UNIMIN CANADA LTD. B GRADE	ELKENM NEFLIN, NORTH CAPE, NORWAY
SiO_2	64.70	63.80	60.2	60.1	55.9
Al_2O_3	20.50	20.90	23.5	23.4	24.2
Fe_2O_3	0.52	0.40	0.08	0.35	0.1
Na_2O	7.62	8.23	10.6	10.5	7.9
K_2O	6.74	6.73	5.1	4.9	9.0
CaO	0.23	0.20	0.3	0.3	1.3
MgO	<0.05	<0.05	trace	trace	trace
TiO_2	<0.01	<0.01	—	—	—
ZrO_2	<0.01	<0.01	—	—	—
P_2O_5	<0.05	<0.05	—	—	0.1
LOI	—	—	0.4	0.3	1.0
TOTAL	100.31	100.26	100.18	99.85	99.5
REFERENCE	McLemore et al. (1996b)	McLemore (1996b)	Guillet (1994)	Guillet (1994)	Guillet (1994)

metals in water samples (Miller, this study) precludes assessment for base metal deposits. Only 13 stream sediment samples were collected from the study area for the U.S. Department of Energy's National Uranium Resource Evaluation (NURE) program and none of the samples had significant anomalies. Reported rock sample data were considered more appropriate indicators of anomalous concentrations of elements. Potential was rated as high, medium, or low, all with moderate to high certainty (Goudarzi, 1984).

Beryllium

A large resource of beryllium occurs at Sierra Blanca Peaks, south of the Cornudas Mountains and within in the Trans-Pecos Texas magmatic province. Cyprus Minerals Inc announced resources totaling 25 million lbs of beryllium oxide grading greater than 2% BeO (Price and others, 1990; Henry, 1992). Beryllium and fluorine derived from intrusions are concentrated in contact limestone. The Tertiary intrusions at Sierra Blanca Peaks are within the alkaline-calcic part of the Trans-Pecos magmatic belt, but are highly evolved two-mica rhyolites that are unique for the province.

Intrusions in the Cornudas Mountains have no potential for Sierra Blanca-type beryllium deposit. This conclusion is based on: 1) the lack of fluorine rich two mica granites, 2) the lack of contact metamorphic aureoles associated with the intrusions.

Rare earth elements and niobium

Rare-earth deposits are typically associated with alkaline rocks, widespread alkali metasomatism, and abundant breccia (Singer, 1986). The intrusions in the Cornudas Mountains have rare-earth enrichment, but only minor altered and brecciated rock. The most altered area in the Cornudas Mountains is in upper Chess Draw, which has been drilled and sampled and evaluated as having no potential (Schreiner, 1994). The potential for undiscovered rare earth and niobium deposits is low to moderate.

Uranium

The potential for uranium deposits in the Cornudas Mountains is low based on low assays in areas of anomalous high radioactivity and the depressed uranium market (McLemore and Chenoweth, 1989; McLemore and Guilinger, 1993).

Gold-silver

Gold-silver deposits in Otero County have been identified as Great Plain margin type (North and McLemore, 1986; 1988) and McLemore (1991, 1996). These deposits in New Mexico are in areas of Tertiary porphyritic alkaline rocks, but the mineralized rock is typically associated with silca-saturated intrusive rocks, and consist of 1) gold-bearing breccia pipes and quartz veins, 2) copper-lead-zinc skarns, and/or 3) iron skarn. Orogrande, about 40 miles (65 km) northwest of the Cornudas Mountains is the largest and most explored deposit of this type.

The Cornudas Mountains have low potential for gold-silver deposits. This assessment is based on the 1) lack of altered and mineralized rock in the Cornudas Mountains, 2) lack of evidence for widespread fluid or vapor phases, 3) lack of silica-saturated rocks (silica saturated rocks present in Great Plain New Mexico model, although are not necessity present in alkaline-related deposits elsewhere) 4) lack of metal enrichment in waters (Miller, this report) or rocks, and 5) lack of faults in sedimentary rock to serve as controlling structures for ore. (Plate 1, this study). The most exposed altered area in the Cornudas Mountains is Chess Draw, which has been drilled and sampled with detection of only trace amounts of gold and silver. There is no indication of a buried metal-enriched porphyry at depth.

Industrial Minerals—nepheline syenite

The Cornudas Mountains have been explored for nepheline syenite for industrial use and a resource is identified at Wind Mountain. Examination of other intrusions in the Cornudas Mountains failed to identify additional nepheline syenite deposits suitable for glass and ceramic use (McLemore and Guilinger, 1993) The potential for an undiscovered resource is low to moderate. The potential for buried syenite of similar composition and texture is moderate to high, but at this time buried intrusions are not a usable source for industrial minerals..

Oil and Gas

The Cornudas Mountains are on the southern edge of the Otero Platform, which was evaluated for oil and gas potential by King and Harder (1985) and Black (1975). They report hydrocarbon shows and drill-stem tests, but none of significance. The most shows have been in Silurian Fusselman Formation and the Permian units, in particular the Abo Formation. Both studies conclude the area has oil and gas potential. The Cornudas Mountains are within an area of oil and gas potential, but are unusual in the occurrence of the intrusive rock. Not only are intrusions exposed, but the widespread folding in the Permian rocks (this study) suggest that intrusive rocks underlie much of the study area. The presence of these intrusives, as well as the implied overmaturity of hydrocarbons, indicate low potential for oil and gas within the study area. Furthermore, neither the Silurian Fusselman nor Abo Formations are present in the subsurface, beneath the Cornudas Mountains (Black, 1975).

REFERENCES

Allen, J.B. and Charsley, T.J., 1968, Nepheline-syenite and phonolite: Institute of Geological Sciences, London, Great Britain, 169 pp.

Anderson, O.J., and Jones, G.E., 1994, Geologic map of New Mexico: New Mexico Bureau of Mines and Mineral Resources Open-File Report 108 A and B, Geologic map and 15 magnetic disks, scale 1:500,000.

Anderson, O.J., Jones, G.E., and Green, G.N, 1997, Geologic map of the Caballo resource area, New Mexico: U.S. Geological Survey Open-File Report OF-97-52, scale:1:500,000.

Bankey, V.L., and Kleinkopf, M.D., 1988, Bouguer gravity anomaly map and four derivative maps of Idaho: U.S. Geological Survey Geophysical Investigations Map GP-978, 3 sheets, scale 1:100,000.

Barker, D. S., 1977, Northern Trans-Pecos Magmatic province: Introduction and comparison with the Kenya rift: Geological Society of America Bulletin, v. 88, p. 1421-1427.

Barker, D. S., and Hodges, F. N., 1977, Mineralogy of intrusions in the Diablo Plateau, northern Trans-Pecos magmatic province, Texas and New Mexico: Geological Society of America Bulletin, v. 88, p. 1428-1436.

Barker, D. S., Long, L. E., Hoops, C. K., and Hodges, F. N., 1977, Petrology and Rb-Sr isotope geochemistry of intrusions in the Diablo Plateau, northern Trans-Pecos magmatic province, Texas and New Mexico: Geological Society of America Bulletin, v. 88, p. 1437-1446.

Barnes, V.E., 1975, Geologic Atlas of Texas, Van Horn-El Paso Sheet, scale 1:250,000

Bauer, P.W. and Lozinski, R.P., 1991, The Bent dome—part of a major Paleozoic uplift in southern New Mexico: *in* J.M. Barker and others, eds., Geology of the Sierra Blanca , Sacramento and Capitan Ranges, New Mexico Geological Society Guidebook 42, p. 175-182

Black, B.A., 1975, Geology and oil and gas potential of the northeast Otero platform area, New Mexico: : *in* W.R. Seager, W.R.,. Clemons,R.E., and Callender, J.F., eds., Las Cruces Country, New Mexico Geological Society Field Conference Guidebook No. 26, Las Cruces County, p. 323-333.

Boggs, R. C., 1985, Mineralogy of the Wind Mountain laccolith, Otero County, New Mexico (abstr.): New Mexico Geology, v. 7, p. 41-42.

Boggs, R. C., 1987, Mineralogy and textures of a eudialyte-bearing dike, Wind Mountain, Otero County, New Mexico (abstr.): New Mexico Geology, v. 9, p. 22.

Boggs, R. C. and Ghose, S., 1985, Georgechaoite, $NaKZrSi_3O_9 \cdot 2H_2O$, a new species from Wind Mountain, New Mexico: Canadian Mineralogist, v. 23, p. 1-4.

Bourne, H. L., 1994, Glass raw materials; in D. C. Carr, ed., Industrial Minerals and Rocks, 6th ed., Society for Mining, Metallurgy, and Exploration, Inc., Ann Arbor, Michigan, pp. 543-550.

Carson Helicopters, Inc., 1981, Residual total intensity magnetic profiles and contour maps, Van Horn quadrangle, Texas: National Uranium Resources Evaluation Project, U.S. Department of Energy, Grand Junction office, Open-File Report GJM-17, scale 1:250,000

Clabaugh, S. E., 1950, Eudialyte and eucolite from southern New Mexico (abstr.): American Mineralogist, v. 35, p. 279-280.

Clabaugh, S.E., 1941, Geology of the northwestern portion of the Cornudas Mountains, New Mexico: unpublished M.S. Thesis, University of Texas at Austin, 66 p.

Collins, G. E., 1958, Preliminary reconnaissance for uranium in the Cornudas Mountains, Otero County, New Mexico and Hudspeth County, Texas: U.S. Atomic Energy Commission, Report DBO-4-TM-5, 16 p.

Cordell, Lindreth, 1983, Composite residual total intensity aeromagmetic map of New Mexico, available from the National Oceanic and Atmospheric Administration (NOAA), National Geophysical Data Center, Code E/GCI, 325 Broadway, Boulder, Co., 80303.

Daly, R.A., 1914, Sills and laccoliths illustrating petrogenesis: International Geological Congress, Canada, 12th Session, Congressional Report, p. 189-204

Dane, C.H., and Bachman, G.O., 1965, Geologic map of New Mexico, U.S. Geological Survey, scale 1:500,000

Foster, R.W., 1978, Oil and gas evaluation of the White Sands Missile Range and Ft. Bliss Military Reservation, south-central New Mexico: New Mexico Bureau of Mines and Mineral resources Open-File report 92, 130 p.

Goudarzi, G.H., compiler, 1984, Guide to preparation of mineral survey reports on public lands: U.S. Geological Survey Open-File Report 84-0787, p. 7, 8.

Geometrics, Inc., 1983, Residual total-intensity magnetic profiles and contour maps, Carlsbad quadrangle, New Mexico: National Uranium Resources Evaluation Project, U.S. Department of Energy, Grand Junction office, Open-File Report GJM-394, scale 1:250,000

Goetz, L.K, 1980, Quaternary faulting in Salt Basin graben, West Texas; *in* Dickerson, P.S., Hoffer, J.M., and Callender, J.F., eds., Trans-Pecos region, southeastern New Mexico and West Texas,: New Mexico Geological Society Thirty-First Field Conference, p. 83-92.

Goetz, L.K., Salt Basin graben: A basin and range right-lateral transtensional fault zone-some speculations, *in* Dickerson, P.W., and Muehlberger, W.R., eds., Structure and tectonics of Trans-Pecos Texas: West Texas Geological Society Publication 85-81, p. 165-168.

Guillett, G. R., 1994, Nepheline syenite; *in* D. C. Carr, ed., Industrial Minerals and Rocks, 6th ed.: Society for Mining, Metallurgy, and Exploration, Inc., An Arbor, Michigan, p. 74-730.

Henry, C.D., 1992, Beryllium and other rare metals in Trans-Pecos Texas: West Texas Geological society Bulletin, v. 31, p. 15.

Hoffman, J.D., and Buttleman, K., 1994, National geochemical database: national uranium resource evaluation data for the conterminous United States: U.S. Geological Survey Digital Data Series DDS-18-A

Holser, W. T., 1959, Trans-Pecos region, Texas and New Mexico; *in* Warner, L. A., Holser, W. T., Wilmarth, V. R., and Cameron, E. N., eds., Occurrence of non-pegmatitic beryllium in the United States: U. S. Geological Survey, Professional Paper 318, 197 p.

Hunt, C.B., 1953, Geology and geography of the Henry Mountains region, Utah: U.S. Geological Survey Professional Paper 228, 234 p.

Industrial Minerals, 1995, Newcomer to nepheline syenite: Industrial Minerals, no. 332, p.17.

Keller, G.R., Veldhuis, J.H., and Powers, D.W., 1983, An analysis of gravity and magnetic anomalies in the Diablo Plateau area, *in* Meader-Roberts, S.J., ed., Geology of the Sierra Diablo and southern Hueco Mountains, West Texas: Permian Basin Section, Society of Economic Geologists and Mineralogists, Field Conference Guidebook, , p. 152-165.

King, P.B., 1934, Permian statigraphy of Trans-Pecos, Texas: Geological Society of America Bulletin , v. 45, p. 697-798

King, W.E., and Harder, V.M., 1985, Oil and gas potential of the Tularosa Basin-Otero platform-Salt Basin graben area, New Mexico and Texas: New Mexico Bureau of Mines and Mineral Resources, Cricular 198, 36 p.

Klein, D.P., and Rodriguez, B.D., 1997, Electrical resistivity survey in the Cornudas Mountains area, Otero County, New Mexico: U.S. Geological Survey Open-File Report 97-149, 25 p.

Kluth, C.F., and Coney, P.J., 1981, Plate tectonics and the ancestral Rocky Mountains: Geology, v. 9, p. 10-15

Korzeb, S.L., and Kness, R.F., 1994, Mineral resources in areas of critical environmental concern in the Caballo Resource area, Otero County, New Mexico: U.S. Bureau of Mines MLA-20-94, 72 p.

Kottlowski, F.E., 1963, Paleozoic and Mesozoic strata of southwestern and south-central New Mexico: New Mexico Bureau of Mines and Mineral Resources Bulletin 79, 100 p.

Kues, B.S., and Lucas, S.G., 1993, Stratigraphy, paleontology and correlation of Lower Cretaceous exposures in southeastern New Mexico; *in* Love, D. L., Hawley, J. W., Kues, B. S., Adams, J. W., Austin, G., S., and Barker, J. M., eds., Carlsbad Region, New Mexico and Texas: New Mexico Geological Society, Guidebook 44, p. 245-260.

Madden, Theodore, and Nelson, Phillip, 1985, A defense of Cagniars's magnetotelluric method: *in* Vozoff, Keeva, ed., Magnetotelluric methods, Geophysics Reprint Series No. 5: Tulsa, Society of Exploration Geophysicists, p. 89-102

Mayer, J.R., 1995, The role of fractures in regional groundwater flow: field evidence and model results from the basin and range of Texas and New Mexico (Ph.D. thesis): University of Texas at Austin, 220 p.

McLemore, V.T., 1983, Uranium and thorium occurrences in New Mexico: distribution, geology, production, and resources; with selected bibliography: New Mexico Bureau of Mines and Mineral Resources, Open-file Report OF-182, 950 p., also; U.S. Department of Energy Report GJBX-11 (83).

McLemore, V. T., 1991, Base- and precious-metal deposits in Lincoln and Otero Counties, New Mexico; *in* Barker, J. M., Kues, B. S, Austin, G. S., and Lucas, S. G., eds., Geology of the Sierra Blanca, Sacramento, and Capitan Ranges, New Mexico: New Mexico Geological Society, Guidebook 42, p. 305-309.

McLemore, V. T., 1996, Great Plains Margin (alkalic-related) gold deposits in New Mexico; *in* Cyner, A. R. and Fahey, P. L., eds., Geology and ore deposits of the American Cordillera: Geological Society of Nevada Symposium Proceedings, Reno/Sparks, Nevada, April 1995, pp. 935-950.

McLemore, V.T., and Chenoweth, W.C., 1989, Uranium resources in New Mexico: New Mexico Bureau of Mines and Mineral Resources, Resource Map 18, 37 p.

McLemore, V. T. and Guilinger, J. R., 1993, Geology of mineral resources of the Cornudas Mountains, Otero County, New Mexico and Hudspeth County, Texas; *in* Love, D. L., Hawley, J. W., Kues, B. S., Adams, J. W., Austin, G., S., and Barker, J. M., eds., Carlsbad Region, New Mexico and Texas: New Mexico Geological Society, Guidebook 44, p. 145-153.

McLemore, V. T. and Guilinger, J. R., 1996, Industrial specifications of the Wind Mountain nepheline syenite deposit, Cornudas Mountains, Otero County, New Mexico; *in* Austin, G.S., Barker, J.M., Hoffman, G., Gilson, N., and Zidec, J., eds., 31st Forum on the Geology of Industrial Minerals, Boderland Forum: New Mexico Bureau of Mines and Mineral Resources, Bulletin 154, in press.

McLemore, V.T., Guilinger, J.R., and Oumiette, M. A., 1994, Geology of the Wind Mountain nepheline syenite deposit, Cornudas Mountains, Otero County, New Mexico: Society Mining, Metallurgy, and Exploration, Preprint 94-63, 10 p.

McLemore, V.T., Lueth, V.W., Guilinger, J.R., and Pease, T.C., 1996a, Geology, mineral resources, and marketing of the Wind Mountain nepheline syenite porphyry, Cornudas Mountains, New Mexico and Texas; *in* Austin, G.S., Barker, J.M., Hoffman, G., Gilson, N., and Zidec, J., eds., 31st Forum on the Geology of Industrial Minerals, Boderland Forum: New Mexico Bureau of Mines and Mineral Resources, Bulletin 154, in press.

McLemore, V. T., Lueth, V. W., Pease, T. C., and Gulinger, J. R., 1996b, Petrology and mineral resources of the Wind Mountain laccolith, Cornudas Mountains, New Mexico and Texas: Canadian Mineralogist, v. 34, pt. 2, p. 335-347.

McLemore, V. T., North, R. M., and Leppert, S., 1988a, REE, niobium, and thorium districts and occurrences in New Mexico: New Mexico Bureau of Mines and Mineral Resources, Open-file Report 324, 27 p.

McLemore, V. T., North, R. M., & Leppert, S., 1988b, Rare-earth elements (REE) in New Mexico: New Mexico Geology, v. 10, p. 33-38.

Miller, W.R., 1997, Environmental geochemistry and processes controlling water chemistry, Cornudas Mountains, New Mexico: U.S. Geological Survey Open-File Report 97-158, 27 p.

North, R. M. and McLemore, V. T., 1986, Silver and gold occurrences in New Mexico: New Mexico Bureau of Mines and Mineral Resources, Resource Map 15, 32 p.

North, R. M. and McLemore, V. T., 1988, A classification of the precious metal deposits of New Mexico; *in* Bulk mineable precious metal deposits of the western United States Symposium Volume: Geological Society of Nevada,, Symposium Proceedings Volume, p. 625–659.

O'Driscoll, M., 1990, U.S. glass industry—over capacity shadows strong demand: Industrial Minerals, p. 34-53.

Potter, M. J., 1990, Annual report of feldspar, nepheline syenite and aplite: U.S. Bureau of Mines, 6 p.

Pray, L.C., 1959, Stratigraphy and structure of the Sacramento Mountains; *in* Sacramento Mountains of Otero County, New Mexico, Permian Basin Section Society of Economic Paleontologists and Mineralogists and the Roswell Geological Society Guidebook, p. 86-130

Pray, L.C., 1988, The western escarpment of the Guadalupe Mountains, Texas and two day field seminar; *in.* Reid, S.T, Bass, R.O., and Welch, Pat, eds., Guadalupe Mountains revisited, Texas and New Mexico, West Texas Geological Society Publication 88-84, p. 23-31

Price, J. G., Henry, C. D., Barker, D. S., and Parker, D. F., 1987, Alkalic rocks of contrasting tectonic settings in Trans-Pecos Texas; *in* Mantle metasomatism and alkaline magmatism: Geological Society of America, Special Paper 215, p. 335-346.

Price, J. G., Rubin, J. N., Henry, C. D., Pinkston, T.L., Tweedy, S.W., and Koppenaal, D. W., 1990, Rare-metal enriched peraluminous rhyolites in a continental arc, Sierra Blanca area, Trans-Pecos Texas;

Chemical modification by vapor-phase crystallization: Geological Society of America, Special Paper 246, p103-120.
Schreiner, R.A., 1994, Mineral investigation of Wind Mountain and the Chess Draw area, Cornudas Mountains, Otero County, New Mexico: U.S. Bureau of Mines MLA 26-94, 46 p.
Singer, D.A., 1986, Descriptive model of carbonatite deposits, in Cox, D.P. and Singer, eds., D.A., Mineral Deposit Models: U.S. Geological Survey Bulletin 1693, p.51-53.
Timm, B. C., 1941, The geology of the southern Cornudas Mountains, Texas and New Mexico: unpublished M.S. thesis, University of Texas at Austin, 55 pp.
Vacquier, V., Steenland, N.C., Henderson, R.G., and Zietz, I., 1951, Interpretation of aeromagnetic maps: Geological Society of America Memoir 47., 151 p.
Wait, J.R., 1962, Theory of magnetotelluric fields: Journal of Research of the National Bureau of Standards-D, Radio Propagation, v. 66D, p. 509-541
Warner, L. A., Holser, W. T., Wilmarth, V. R., & Cameron, E. N., 1959, Occurrence of nonpegmatite beryllium in the United States: U.S. Geological Survey, Professional Paper 318, 198 p.
Woodward, L.A., Callender, J.F., Gries, J., Seager, W.R., Chapin, C.E., Zilinski, R.E., and Schaffer, W.L., 1975, Tectonic map of the Rio Grande region, Colorado-New Mexico border to Presidio, Texas; *in* W.R. Seager, W.R., Clemons, R.E., and Callender, J.F., eds., Las Cruces Country, New Mexico Geological Society Field Conference Guidebook No. 26, p. 239
Zapp, A. D., 1941, Geology of the northeastern Cornudas Mountains, New Mexico: unpublished M.S. Thesis, University of Texas at Austin, 63 pp.